



**SIMULATION IN ADVANCED
HEART FAILURE WITH A
VIEW TO SELECTION AND
OPTIMIZATION OF DEVICE
THERAPY**

**SARA SALTAROCCHI
M.D.**

**Sapienza University of Rome
Faculty of Pharmacy and Medicine
Degree Course “F” in Medicine and Surgery**

**Department of Cardiovascular, Respiratory,
Nephrological, Anaesthetic and Geriatric Sciences**

**Institute of Clinical Physiology
National Research Council of Italy (Rome)**

SEPTEMBER 2018

Acknowledgement

I would like to thank my supervisor, Prof. Iginio Genuini, for proposing me this thesis and the collaboration with the Institute of Clinical Physiology (National Research Council - CNR). I am truly grateful to my co-supervisor, Dr. Eng. Claudio De Lazzari, who gave me the chance to work in the Cardiovascular Numerical/Hybrid Modelling Lab and guided me in every step of my research throughout the year, teaching me a new approach that I believe will be crucial in my educational background as a physician. I would also like to thank Dr. Massimo Capoccia for all his suggestions and for helping me with language editing. I am also thankful to Prof. Massimo Mancone for the final editing of this piece of work. A special mention to my brother Luca, my parents and my lifelong friends for the endless support given during my studies.

ABSTRACT

Ventricular Assist Devices (VADs) are mechanical pumps designed to provide hemodynamic support in patients with advanced heart failure; the introduction of VADs has revolutionized heart failure management, providing increased functional capacity and quality of life for patients. Simulation is an educational method based on virtual reproduction of real or close to real life situations. Modelling and simulation may become clinically applicable tools for detailed evaluation of the cardiovascular system and clinical decision-making to guide therapeutic intervention. What we propose is the use of a simulation approach for the optimization of device-based treatment, in order to guide therapeutic intervention in advanced heart failure. The aim of this study is to compare the outcome of the simulations with the previously made clinical decisions in order to find out any relationship that may be applicable on a routine basis in future patient assessment. Simulations were carried out using the software CARDIOSIM[®], a numerical simulator of the cardiovascular system. Different mechanical circulatory support systems have been implemented in the simulator in order to study the interaction between assist devices and the cardiovascular system in terms of hemodynamic and ventricular energetic parameters; the VAD that was used and integrated in the software is the Berlin Heart INCOR[®] Pump.

The outcome of the simulations showed results that are consistent with the decisions made by Multidisciplinary Team Meetings (Scottish National Advanced Heart Failure Service, Glasgow, UK).

Statistical Analysis performed through Student's t-test and Mann-Whitney test overall confirmed the accuracy of CARDIOSIM[®] in reproducing the different hemodynamic parameters. The outcome of the simulations addressed the value of a more quantitative approach in the clinical decision process.

Despite the preliminary nature of this study and the limited number of patients considered, CARDIOSIM[®] has the potential to deliver reliable simulations for a more quantitative and critical evaluation of device/drug treatment and optimization in advanced heart failure. The clinician remains the ultimate decision-maker but relies on an additional tool that may reduce unnecessary guess work and uncertainty.

CONTENTS

<u>CHAPTER</u>	<u>PAGE</u>
ACKNOWLEDGEMENT	1
ABSTRACT	2
1 INTRODUCTION	9-20
1.1 Overview on Heart Failure	
1.2 Patient Selection for LVAD implantation	
1.3 Type of Devices	
1.4 Simulation in Healthcare education	
2 AIM OF THE STUDY	21
3 MATERIALS AND METHODS	22-35
3.1 A Lumped-parameter Model of the Cardiovascular System	
3.2 Ventricular and Atrial Numerical Modelling	
3.3 Berlin Heart INCOR [®] Pump	
3.4 Patient Analysis and Simulations	
3.4.1 Patient #1	
3.4.2 Patient #2	
3.4.3 Patient #3	
3.4.4 Patients #4, #5 and #6	

4	RESULTS	36-51
	4.1 Patient #1	
	4.2 Patient #2	
	4.3 Patient #3	
	4.4 Patient #4	
	4.5 Patient #5	
	4.6 Patient #6	
	4.7 Discussion	
5	STATISTICAL ANALYSIS	52-54
6	CONCLUSIONS	55
	REFERENCES	56-62

LIST OF TABLES

TITLE

NYHA Classification

ACC/AHA Classification

Setting parameters of the Berlin Heart Incor® Pump

Hemodynamic data of Patient #1 on Admission and after 4 days

Hemodynamic data of Patient #2 on Admission and after 1 and 2 months

Hemodynamic data of Patient #3 on Admission and after 15 and 22 days

Hemodynamic data of Patients #4, #5 and #6 on Admission

Measured parameters and simulation results for Patient #1

Measured parameters and simulation results for Patient #2

Measured parameters and simulation results for Patient #3

Measured parameters and simulation results for Patient #4

Simulation results with Milrinone for Patient #4

Measured parameters and simulation results for Patient #5

Simulation results with Milrinone for Patient #5

Measured parameters and simulation results for Patient #6

Simulation results with Milrinone for Patient #6

LIST OF FIGURES

TITLE

- Starling curves representing a normal and a failing heart
- Algorithm for Stage D HF_rEF
- Electrical analogue of the cardiovascular system
- Schematic representation of the ECG signal
- Berlin Heart INCOR[®] Pump
- Berlin Heart INCOR[®] Pump. Battery, driving unit and bag
- Electrical analogue of Berlin Heart INCOR[®] Pump
- Left Ventricular Loop in the PV plane
- Screen output obtained from CARDIOSIM[®] for Patient #2
- Screen output obtained from CARDIOSIM[®] for Patient #4
- Graphical representation of the left ventricular PV loops in Patient #5
- Graphical representation of PV loops in Patient #6
- Graphical representation of CBF in Patients #4, #5 and #6
- Screen output obtained from the software Stata[®] for LVEF%
- Comparison between measured and simulated LVEF% values

LIST OF ABBREVIATIONS

ACC	American College of Cardiology
ACCF	American College of Cardiology Foundation
ACEI	Angiotensin – Converting Enzyme Inhibitor
ADL	Activities of Daily Living
AHA	American Heart Association
ANP	Atrial Natriuretic Peptide
BNP	Brain Natriuretic Peptide
BP	Mean Blood Pressure
BSA	Body Surface Area
BTD	Bridge to Decision
BTT	Bridge to Transplant
CBF	Coronary Blood Flow
CO	Cardiac Output
CO_{VENTR}	Left Ventricular Output Flow
CI	Cardiac Index
CRT	Cardiac Resynchronization Therapy
DT	Destination Therapy
Ea	Arterial Elastance
EDPVR	End - Diastolic Pressure - Volume Relationship
EDV	End Diastolic Volume
Ees	Ventricular Elastance
ESPVR	End - Systolic Pressure - Volume Relationship
ESV	End Systolic Volume
HF	Heart Failure
HF_nEF	Heart Failure with normal Ejection Fraction
HF_pEF	Heart Failure with preserved Ejection Fraction
HF_rEF	Heart Failure with reduced Ejection Fraction
HFSS	Heart Failure Survival Score
HM II	HeartMate II Left Ventricular Assist Device
HR	Heart Rate
IABP	Intra-Aortic Balloon Pump
ICD	Implantable Cardioverter Defibrillator
IFC - CNR	Institute of Clinical Physiology - National Research Council of Italy
INTERMACS	Interagency Registry for Mechanically Assisted Circulatory Support
IV	Intravenous
LAD	Left Anterior Descending Coronary Artery

LV	Left Ventricle
LVAD	Left Ventricular Assist Device
LVEDP	Left Ventricular End - Diastolic Pressure
LVEF	Left Ventricular Ejection Fraction
MAP	Mean Arterial Pressure
MCSS	Mechanical Circulatory Support System
MDT	Multidisciplinary Team
MRA	Mineralocorticoid Receptor Antagonist
NYHA	New York Heart Association
PA	Pulmonary Arterial
PCI	Percutaneous Coronary Intervention
PCWP	Pulmonary Capillary Wedge Pressure
PDE3	Phosphodiesterase 3
PES	End – Systolic Pressure
PLA	Left Atrial Pressure
PV	Pressure - Volume
PVR	Peripheral Vascular Resistance
Q_{TOT}	Total cardiac output ($Q_{TOT}=CO_{VENTR}+Q_{VAD}$)
Q_{VAD}	LVAD Output Flow
RA	Right Atrial
RV	Right Ventricular
RAAS	Renin – Angiotensin – Aldosterone System
REMATCH	Randomized Evaluation of Mechanical Assistance for the Treatment of Congestive Heart Failure
RHC	Right Heart Catheterization
ROADMAP	Risk Assessment and Comparative Effectiveness of Left Ventricular Assist Device and Medical Management in Ambulatory Heart Failure Patients
RVSWI	Right Ventricular Stroke Work Index
SHFM	Seattle Heart Failure Model
SV	Stroke Volume
TAPSE	Tricuspid Annular Plane Systolic Excursion
TPG	Transpulmonary Gradient
VAD	Ventricular Assist Device

Chapter 1: INTRODUCTION

Ventricular Assist Devices (VADs) are mechanical pumps designed to provide hemodynamic support in patients with advanced heart failure with a view to recovery, bridge to transplant or long-term treatment. VADs have revolutionized advanced heart failure management providing meaningful increase in functional capacity and quality of life for patients. Since the Randomized Evaluation of Mechanical Assistance for the Treatment of Congestive Heart Failure (REMATCH) Trial [80][81], the technological development from pulsatile to continuous-flow ventricular assist devices has led to an increased survival of patients on prolonged circulatory support [9][48][77][87]. In patients up to 70 years of age without cardiogenic shock, diabetes and renal failure, mechanical circulatory support with a continuous-flow left ventricular assist device (LVAD) has shown 1- and 2-year survival of 80% and 70%, which is comparable with heart transplantation [47][48]. A recent analysis has reported greater durability for continuous-flow left ventricular assist devices in comparison with pulsatile-flow devices [40] and confirmed its increasing trend [73]. Despite the highly sophisticated technology and the key role played by LVAD treatment in advanced heart failure, there are still unresolved issues which are currently being addressed [26][83].

1.1 Overview on Heart Failure

Despite advances in medical treatment, heart failure remains a healthcare burden with significant morbidity and approximately 50% mortality within 5 years of diagnosis [37][73]. The high prevalence of well-known risk factors such as hypertension, diabetes, metabolic syndrome and atherosclerotic disease [102] requires a more targeted focus on those patients who are at higher risk for the development of heart failure. The ACCF/AHA guidelines consider patients with a left ventricular ejection fraction (LVEF) $\geq 50\%$ as showing a preserved systolic function [102] with previous findings suggesting that asymptomatic patients with LVEF $< 50\%$ are at greater risk for the development of heart failure [95][96][103]. Considering that the “normal” classification for LVEF is within the 55% to 65% range and an increased heart failure risk is observed with a LVEF $< 50\%$, the question is whether there is an increased risk among patients who fall in the 50% to 55% range [36]. Perhaps the treatment of patients with “borderline” or “low normal” LVEF may need to be re-evaluated in view of the misleading nature of these terms and the fact that these patients remain at increased risk of developing heart failure in the light of more recent evidence [92].

The relationship between form and function determines cardiac performance. Impaired adaptation of form to function in a failing heart leads to either systolic (impaired contractility and ejection) or diastolic (impaired relaxation and filling) heart failure, which are currently defined in terms of ejection fraction: heart failure with reduced ejection fraction (HFrEF) and heart failure with normal or preserved ejection fraction (HFpEF or HFpEF). HFrEF consists of left ventricular dilatation due to increased cardiac myocyte length because of sarcomere addition in series leading to accept greater venous return at the expense of increased energy cost of ejection. HFpEF consists of left ventricular hypertrophy due to increased myocyte thickness secondary to sarcomere addition in parallel facilitating ejection but with impaired filling [43]. As a consequence, heart failure can be defined as a clinical syndrome with reduced cardiac output and increased venous pressures accompanied by molecular

abnormalities, which cause progressive deterioration of the failing heart and premature myocardial cell death [44]. More recently, an integrative approach that goes beyond ejection fraction has been advocated for the assessment of cardiac structure and function in heart failure [13].

The signs and symptoms of heart failure (HF) are the result of the clinical sequelae of inadequate cardiac output (CO) and lack of efficient venous return. Dyspnoea, cough, and wheezing are the result of increased pressure in the pulmonary capillary bed due to ineffective forward flow from the left ventricle. Lower extremity oedema and ascites occur when the right ventricle is unable to accommodate the systemic venous return. Fatigue is common as the failing heart cannot sustain enough CO to meet the body's metabolic requirements with particular reference to heart and brain. Nausea and lack of appetite may also occur as blood is shifted from the gastrointestinal tract to the more vital organs. Palpitations can occur as the failing heart tries to accommodate for the lack of flow with a faster heart rate.

The New York Heart Association (NYHA) classification system is widely used for the assessment of patients in heart failure according to their symptoms (Table 1).

Table 1 NYHA classification

NYHA Classification	
Class I	No symptoms with ordinary activity. Ordinary physical activity does not cause undue fatigue, palpitation, dyspnea or angina.
Class II	Slight limitation of physical activity. Comfortable at rest, but ordinary physical activity results in fatigue, palpitation, dyspnea or angina.
Class III	Marked limitation of physical activity. Comfortable at rest but less than ordinary physical activity results in fatigue, palpitation, dyspnea or angina.
Class IV	Unable to carry out any physical activity without discomfort. Symptoms of cardiac insufficiency may be present even at rest.

The NYHA class system is also used as an entry criterion and an outcome measure for clinical trials of medications and devices [6][58]. More recently, a new system has been introduced by the American College of Cardiology (ACC) and the American Heart Association (AHA) that emphasizes both the evolution and progression of the disease (Table 2) in the context of established risk factors as well as structural features for the development of HF [102].

Table 2. ACC/AHA classification.

ACC/AHA Classification	
Stage A	Patient at high risk for developing HF with no structural disorder of the heart.
Stage B	Patient with structural disorder of the heart without symptoms of HF.
Stage C	Patient with past or current symptoms of HF associated with underlying structural heart disease.
Stage D	Patient with end-stage disease who requires specialized treatment strategies.

The leading cause of HF with reduced ejection fraction (HFrEF) is the loss of functional myocardium due to ischemic disease and infarction; volume overload due to valvular incompetence and impaired contractility from cardiotoxins and cardiotoxic drugs are also contributors. The consequence of LV dysfunction is decreased CO which in turn leads to global hypoperfusion. In addition, LV dysfunction causes an increase in the amount of blood in the ventricle and therefore an increase in both end-systolic and end-diastolic volumes. This in turn leads to an increase in LV end-diastolic pressure (LVEDP), which causes elevated left atrial pressure leading to increased pulmonary capillary pressure with congestion and onset of dyspnoea. Left ventricular failure is also the most common cause of right ventricular failure, which leads to elevated right atrial pressure with impaired venous drainage due to increased pressure in the vena cava system. This leads to increased pressure in the liver, the gastrointestinal tract and the lower extremities with clinical signs and symptoms of abdominal pain, hepatomegaly, and peripheral oedema. Compensatory attempts such as Frank-Starling mechanism, neuro-hormonal activation and ventricular remodelling will maintain mean arterial pressure (MAP) and tissue perfusion although their long-term effects will generate a vicious cycle with worsening of heart failure.

Figure 1 describes hypothetical Starling curves where a normal heart operates on the ascending limb of the curve (Point A) and a failing heart on the descending limb of a depressed curve (Point B).

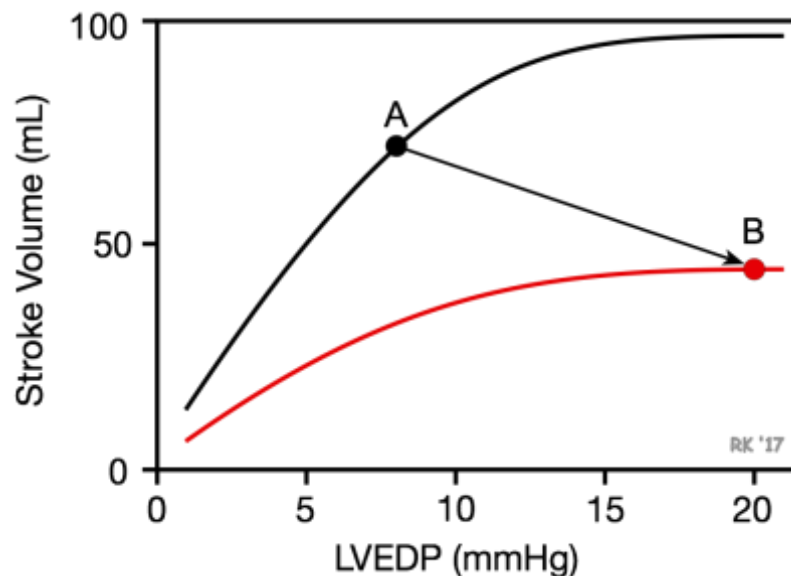


Fig. 1 Starling curves representing a normal and a failing heart

The activation of the renin-angiotensin–aldosterone system (RAAS) causes vasoconstriction and sodium retention to maintain MAP. The atrial natriuretic peptide (ANP) and brain natriuretic peptide (BNP) are released respectively by atria and ventricles in response to myocardial stretch and act directly on blood vessels to cause vasodilatation, salt and water excretion, and inhibit secretion of renin, aldosterone, and vasopressin. Elevated BNP in particular is thought to be one of the first signs of HF and is used to follow the progression of disease. In addition, endothelium-derived vasoactive substances also play a role.

The hemodynamic events described lead to cardiac remodelling with changes in size, shape, structure, and function of the left ventricle. The loss of its elliptical conformation in exchange of a more spherical one is an initial compensatory attempt to increase ventricular volume, which leads to greater stroke volume (SV) and higher CO to overcome a reduced left ventricular ejection fraction (LVEF). Myocardial wall thickness and overall ventricular mass are also increased in an attempt to enhance contractility. Further ventricular dilatation and myocardial hypertrophy lead to increased wall tension and fibrosis with progressive functional impairment, onset of dyssynchrony, multi-organ failure and myocardial apoptosis on the long term.

Traditionally, the mainstay of treatment has always been neurohormonal blockade by means of angiotensin converting enzyme inhibitors (ACEIs), mineralocorticoid receptor antagonists (MRAs), beta-blockers and diuretics. Digoxin may also be used accordingly. Treatment with the sinus-node inhibitor Ivabradine, which reduces heart rate acting on I_f -channels, seems to reduce hospital admission for worsening HF [90]. More recently, LCZ696, which combines an angiotensin II inhibitor with a neprilysin inhibitor, may have some potential for HFrEF patients [65].

Biventricular pacing has shown improved survival, reverse remodelling, and improved quality of life in a selected group of patients [46]. Palliation with continuous intravenous (IV) inotropes remains the only option for many Stage D HFrEF patients, who are not eligible for transplant or too sick for LVAD insertion [62].

A therapeutic algorithm for Stage D HF_rEF is shown in Fig. 2 [59] although further review may be needed in the near future according to the 2013 guidelines of the International Society for Heart and Lung Transplantation [32].

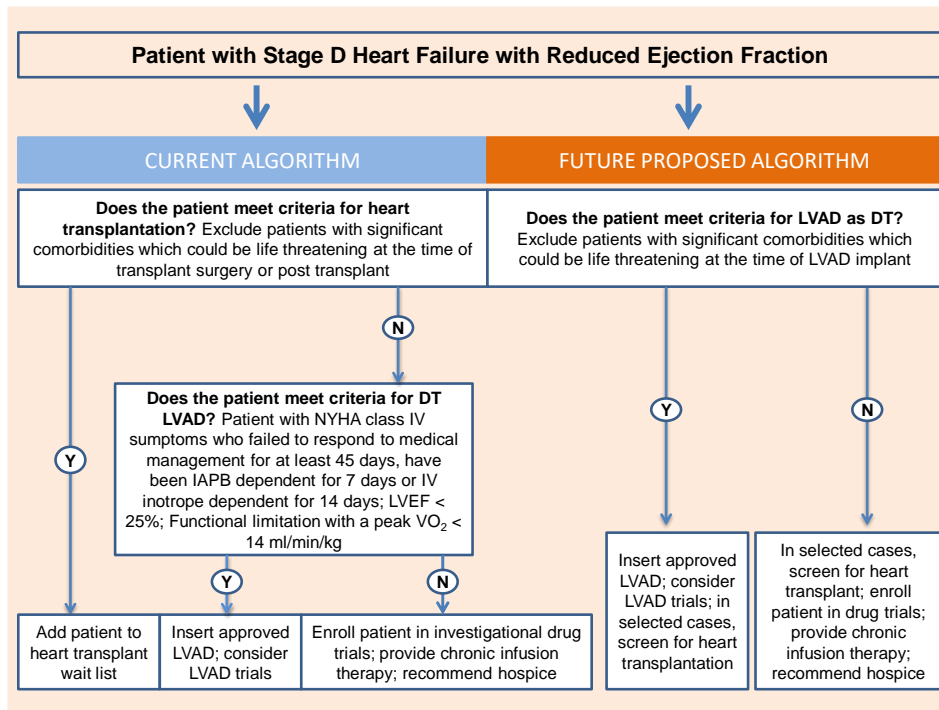


Fig. 2 Algorithm for Stage D HF_rEF

Left ventricular unloading following LVAD insertion results in decreased left ventricular work, reduces myocardial damage, improves chamber compliance, and favours “reverse remodelling” with improved hemodynamic and functional status [28]. A reduction in pulmonary pressures and trans-pulmonary gradient is an indication for transplant candidacy [67].

1.2 Patient selection for LVAD implantation

Patient selection and timing of implant remain key factors for successful LVAD treatment. Assessment for the appropriateness of LVAD support should be based on the degree of disease; ability to undergo the operation successfully; ability to be discharged home with adequate family support for long-term success. Risk factors for poor survival should be identified and treated whenever possible to minimize their effect [86].

Traditionally, LVAD insertion was considered for younger patients as a bridge to transplant (BTT) [70]. Following the REMATCH trial, a growing number of advanced heart failure patients non-eligible for transplantation underwent LVAD insertion for prolonged support or destination therapy (DT). Another indication is bridge to decision (BTD) for those patient with relative contra-indications to transplantation that may be reversible after a prolonged period of hemodynamic support.

Although there are established guidelines for heart transplantation [66], there are no universally accepted criteria for LVAD implantation [32][79][102].

At present, LVAD insertion remains an elective procedure with prognostic indication in selected patients with advanced stage D HFrEF refractory to optimal medical treatment and cardiac device intervention [100]. Frequently used indicators of illness severity are those following the REMATCH and HM II Destination Therapy Trials [70][80][87]:

- Patients with NYHA functional class IV symptoms who have failed to respond to optimal medical management, including angiotensin-converting enzyme inhibitors or beta-blockers, for at least 45 of the past 60 days, or have been intra-aortic balloon pump (IABP)-dependent for 7 days or IV inotrope-dependent for 14 days;
- Left ventricular ejection fraction <25%;
- Functional limitation with a peak oxygen consumption <14 ml/kg/min, unless on an intra-aortic balloon pump, IV inotropes, or physically unable to perform the exercise test.

Eligibility for heart transplant remains an important consideration for LVAD insertion although there are some key elements to consider: pulmonary hypertension or recent cancer are relative contra-indications for heart transplantation but not for LVAD insertion, whereas complex congenital heart disease or significant right ventricular failure are not optimal for LVAD insertion but may benefit from heart transplantation [38].

Although LVAD insertion was previously restricted to patients with a body surface area BSA > 1.5 m², the availability of continuous-flow rotary blood pumps has overcome this limitation, in contrast to heart transplantation where most programs limit donors to ± 15% of the recipient's weight [14]. Important contraindications include: systemic illness with a life expectancy of less than 2 years or with multi-organ involvement; irreversible renal, hepatic or neurological disease; severe obstructive pulmonary disease; severe psychosocial limitation or medical non-adherence; malignancy within 5 years although LVAD may be an acceptable option for a patient with a potentially curable cancer who is unable to survive the 5-year disease-free interval required for heart transplantation. Similarly, active systemic infection, prolonged intubation, age > 80 years, obesity or malnutrition, and musculoskeletal diseases that could impair rehabilitation are relative contraindications that may not preclude patients from receiving a LVAD [14]. Assessment of right ventricular function plays a key role in decision-making for LVAD insertion because right ventricular failure remains a major contributing factor to postoperative bleeding, renal failure, need for right ventricular support and prolonged hospital stay [86]. Although echocardiographic parameters such as tricuspid annular plane systolic excursion (TAPSE) are still being used, its validity remains questionable whereas right ventricular stroke work index (RVSWI) through right heart catheter is currently the parameter of choice [34][52][63].

Although widely and successfully used in clinical practice, the NYHA classification of clinical status remains inadequate for the selection and treatment of patients in advanced heart failure. The Heart Failure Survival Score [1] and the Seattle Heart Failure Model [55]

can be used to estimate the expected survival during the first two years on medical treatment and identify those patients at high risk of death who may benefit from LVAD support. These patients can be stratified into high, medium and low risk for LVAD support [54].

The Heart Failure Survival Score (HFSS) is a clinical decision-making prognostic tool for ambulatory patients with advanced heart failure. It is a non-invasive risk stratification model aimed at the selection of candidates for cardiac transplantation. Its suboptimal predictive accuracy in some validation data sets has led to the development of the Seattle Heart Failure Model (SHFM) [55].

The SHFM is a multivariate risk model, which identifies certain variables as significant predictors of survival. The model gives an accurate estimate of 1-, 2-, and 3-year survival based on easily obtained clinical, pharmacological, device and laboratory data. The SHFM has been recently updated to allow application to higher risk hospitalized patients by including iv diuretics, inotropic support, IABP, ventilator, ultrafiltration, the use of newer LVADs and the use of updated guidelines for ICD/CRT/CRT-D2 [2][45][54][55][56][94]. These changes have also been used in the ROADMAP LVAD trial. In addition, the AHA/ACC Heart Failure Guidelines state that "validated multivariable risk scores can be useful to estimate subsequent mortality risk in ambulatory or hospitalized patients with heart failure" (Class IIa) [100][102].

Patients considered for mechanical circulatory support can be classified according to the profiles developed from the data collected for the Interagency Registry for Mechanically Assisted Circulatory Support (INTERMACS) that can help identify risks related to the timing of LVAD insertion [48][87]. The profile classification is as follows:

Profile 1: Cardiogenic shock

Patients with life-threatening hypotension despite rapidly escalating inotropic support and critical organ hypoperfusion, often confirmed by worsening acidosis and/or lactate levels. Definitive intervention is needed within hours.

Profile 2: Progressive decline

Patients with declining function despite intravenous inotropic support may be manifest by worsening renal function, nutritional depletion and inability to restore volume balance. Also, declining status in patients unable to tolerate inotropic therapy. Definitive intervention is needed within few days.

Profile 3: Stable but inotrope dependent

Patients with stable blood pressure, organ function, nutrition and symptoms on continuous intravenous inotropic support (or a temporary circulatory support device or both), but showing repeated failure to wean from support due to recurrent symptomatic hypotension or renal dysfunction. Definitive intervention is elective over a period of weeks to few months.

Profile 4: Resting symptoms

Patients can be stabilized close to normal volume status but experience daily symptoms of congestion at rest or during activities of daily living (ADL). Doses of diuretics generally fluctuate at very high levels. More intensive management and surveillance strategies should be considered, which may reveal poor compliance in some cases that would compromise outcomes with any treatment. Some patients may shuttle between 4 and 5. Definitive intervention is elective over a period of weeks to few months.

Profile 5: Exertion intolerant

Patients comfortable at rest and with activities of daily living (ADL) but unable to engage in any other activity and living predominantly within their home environment. Patients are comfortable at rest without congestive symptoms, but may have underlying refractory elevated volume status, often with renal dysfunction. If underlying nutritional status and organ function are marginal, patients may be more at risk than INTERMACS 4 and require definitive intervention. Variable urgency of intervention, which depends upon maintenance of nutrition, organ function and activity.

Profile 6: Exertion limited

Patients without evidence of fluid overload who are comfortable at rest, with activities of daily living and minor activities outside their home environment but fatigue after the first few minutes of any meaningful activity. Attribution to cardiac limitation requires careful measurement of peak oxygen consumption, in some cases with hemodynamic monitoring to confirm severity of cardiac impairment. Variable urgency of intervention, which depends upon maintenance of nutrition, organ function and activity.

Profile 7: Advanced NYHA III

Patients who are without current or recent episodes of unstable fluid balance, living comfortably with meaningful activity limited to mild physical exertion. Transplantation or circulatory support may not currently be indicated.

Outcomes for LVAD insertion are inferior for INTERMACS 1-2 patients for whom temporary extra-corporeal mechanical circulatory support is an appropriate strategy to achieve clinical stability and proceed to long-term LVAD insertion in a more elective manner. INTERMACS 3 patients have been traditionally considered as the optimal group for long-term LVAD insertion [38]. Retrospective analyses suggest that survival is even better in non-inotrope-dependent patients [9][42] and the prospective ROADMAP study has shown superior outcome in INTERMACS 4-7 patients compared to full medical treatment [31]. In summary, long-term LVAD insertion should be considered in selected INTERMACS 1-2 patients, in every INTERMACS 3 patient and in severely symptomatic and motivated INTERMACS 4-7 patients who are prepared to accept a risk of adverse events in exchange for longer survival and better functional capacity [38].

Although pre-operative scoring systems to predict outcome following LVAD insertion, such as the DT and HeartMate II risk score, have been proposed and tested in prospective studies [15][91], they should not be considered as the only tool for patient selection.

Identification of patients with early advanced heart failure remains challenging and early referral for further evaluation in a LVAD or transplant centre is essential. Patients who remain in NYHA III despite full medical treatment and cardiac resynchronization therapy (CRT) should be referred or at least discussed if needed [38].

1.3 Type of Devices

Essentially, there are two main categories of mechanical blood pumps: volume-displacement and rotary pumps.

Volume-displacement pumps are known as first generation devices. They consist of a chamber or a sac that fills passively or by suction and is compressed by an external pusher plate. Energy is transferred to the blood by periodic changes in a working space generating pulsatile flow in an attempt to emulate the natural behaviour of the heart. Inflow and outflow prosthetic valves are needed to maintain unidirectional flow. Novacor and HeartMate I XVE devices were developed based on this principle. The driving source can be air (pneumatic system), an incompressible fluid (electro-hydraulic mechanism), a magnet (electromagnetic system) or an electric drive unit (electro-mechanic system). A pulsatile LVAD can operate “in phase” and “out of phase” with the native heart [8][64]. When LVAD-heart coupling is in phase, ventricular systole occurs during LVAD diastole resulting in highest filling of the device with decreased left ventricular pressure. When LVAD-heart coupling is out of phase, the two pumps are in competition resulting in decreased device filling and increased left ventricular pressure. The in phase mode achieves a more controlled ability to partially unload the native heart with potential for myocardial recovery [8][30]. In addition, the in-phase mode increases diastolic aortic pressure with significant improvement of coronary perfusion because LVAD systole occurs during left ventricular diastole (counterpulsation). The output requirement for a pulsatile configuration is a flow rate of 5-10 L/min at a mean pressure of 100-150 mmHg and a rate less than 120 bpm with a mean filling pressure of about 20 mmHg [3]. Although volume-displacement pumps generate pulsatile flow and unload the left ventricle very efficiently, there are clear disadvantages such as large size, complexity, noisy operating mode and limited durability because of many moving parts [5][75].

Rotary blood pumps have an inlet and an outlet with a single rotating element, the impeller, which transfers energy to the blood in order to increase arterial blood flow and pressure. Energy is transmitted by the impeller’s vanes through velocity changes, generating a continuous, non-pulsatile flow. These devices can be axial, centrifugal or diagonal according to the geometry of the impeller: axial flow pumps have a cylindrical rotor with helical vanes causing the blood to accelerate in the direction of the rotor’s axis; in centrifugal flow pumps, the blood is accelerated circumferentially with movement towards the external rim of the pump. Rotary pumps are suitable for high flows up to 20L/min at differential pressures lower than 500 mmHg. The centrifugal design can produce high pressures and low flows. An axial flow pump generates high flows at low pressure differences. A diagonal pump is a mixed flow system capable of generating high pressures and high flows [85]. Axial flow pumps like HeartMate II and Jarvik 2000 requiring mechanical bearings and seals in contact with blood are known as second generation devices. They are smaller, easy to insert and more durable because of a single moving part. Although thrombus formation remains a serious

complication, experience with this type of devices is well established [70][76][84][86]. Centrifugal flow pumps like HeartWare, DuraHeart and HeartMate III based on magnetic levitation or non-contacting hydrodynamic bearings are known as third generation devices. These pumps are even smaller and the use of magnetically levitated rotor systems is likely to improve durability. Early results are promising and their use is increasing [72][74][89][93][97]. The MOMENTUM-3 trial will be even more specific on the performance and future of the HeartMate III [39].

Volume-displacement pumps generate pressure against resistance like the human heart, which can be considered as a modified and more complex volume displacement pump. They maintain a constant flow against an increasing resistance, thereby generating a greater pressure at the expense of increased work and energy consumption. However, at very high resistance (e.g. aortic clamping) the pump fails. In contrast, rotary pumps generate flow with an amount of pressure depending on resistance to flow. If the aorta is clamped, although the impeller seems to be pushing against an infinite resistance, the actual work of the pump decreases. The rotor maintains the same rotational speed but the impeller contacts and “thrusts” less fluid and, thus, does less work. In summary, the main difference between the two pumps is that the rotary one can handle a low/no flow event very well by reducing its workload rather than increasing it like a volume displacement pump does. This could be also important for device monitoring: if the controller shows decreased power usage with a stable rotor speed, this implies decreased work and, thus, decreased flow. This could result from decreased inflow due to volume depletion or cannula malposition or from increased afterload due to vasoconstriction, hypertension, or cannula geometry [4].

1.4 Simulation in Healthcare Education

Simulation is an educational method based on virtual reproduction of real or close to real life situations. A simulator allows the operator to reproduce phenomena likely to occur in daily clinical practice under controlled conditions [24]. The importance of simulation is confirmed by the score (in percentage) gained according to the “learning pyramid” in comparison with other educational tools: its location is between “demonstration” and “practice doing”. The opportunity to reproduce a situation and analyse all the relevant variables and parameters gives additional insights to medical education that cannot be achieved by theory and discussion only. Repetition of a specific process or situation in a controlled environment may help consolidate knowledge retention and procedure sequence with immediate feedback. The ability to predict outcome following intervention in a controlled environment may help treatment optimization with potential for clinical application. Besides, simulation may become a tool for the development and reinforcement of standards in clinical practice through analysis and repetition in the light of Aristotle’s statement: “We are what we repeatedly do. Excellence then is not an act but a habit.”

There has been an exponential growth in the adoption of simulation in healthcare education internationally over the past two decades with growing acceptance as an educational method aimed at patient’s safety. Close relationship between theory and practice is widely acknowledged in medical practice. An apprenticeship learning style has been traditionally followed to achieve the required skills to practice as a physician or surgeon based on the

known principle “See One, Do One, Teach One”. Although effective, this approach has been challenged in more recent years in view of the significant changes in the healthcare system including availability of resources, restriction of junior doctors’ hours, variability of training programs, evidence-based medicine approach, clinical governance, surgeon-specific results. Although controversy remains, there have been studies showing concerns for the skills level of medical graduates, even in western countries [53]. Simulation in healthcare has been driven by patients’ safety. Medical errors cause injury to about 3% of hospitalized patients, resulting in more than 44000 deaths per year in the USA [50]. Simulation in a controlled environment may help reduce the potential for error through the development of specialty-specific skills according to certain requirements.

A close cooperation between clinicians and engineers remains a key element for the development of simulation environments as close as possible to real life situations in an attempt to achieve the desired outcome. Essentially, three types of simulators are available. Low-fidelity simulators lack realism or situational context and for this reason they are mainly used for the training of basic skills; an example is the Resusci-Anne manikin. Moderate-fidelity simulators offer limited but more plausible scenarios with elements like pulse, heart sounds, breathing sounds, which can be used to acquire basic and more advanced skills; an example is Harvey simulator. High-fidelity simulators consist of highly sophisticated manikins where interventional procedures with increasing degree of complexity can be performed; an example is the SimMan manikin.

The main purpose of simulation in specialty-specific training is:

- Learning of complex and/or invasive procedures through skill- or task-repetition without any risk for the patient;
- Revision of diagnostic and therapeutic approach through micro-simulation programs consisting of clinical scenarios;
- Acquisition of specific skills for the management of complex clinical cases or critical situations through role-playing using high-fidelity systems;
- Interactive learning of algorithms for the management of complex clinical situations;
- Maintain the ability to perform a procedure smoothly following repeated exposure and feedback;
- Maintain the ability to a problem-solving approach following exposure to different simulated clinical conditions;
- Use of familiar and non-familiar pharmacological and/or procedural therapeutic approaches during the simulations in order to evaluate risk and benefits of each choice.

Currently in the USA, Australia and Europe, a simulation-based approach is widely used in the field of medicine and surgery to integrate traditional training programs and Continuing Medical Education. Many healthcare centres around the world are using complex mathematical models that mimic clinical problems often encountered in clinical practice. In Italy, in particular, a cardiovascular software simulator named CARDIOSIM[®] is being used for the training of students in medicine, bioengineering and clinical engineering, and also for the purposes of continuing medical education (CME) [23][24]. CARDIOSIM[®] is a modular software simulation system developed by the Cardiovascular Numerical/Hybrid Modelling

Lab based in Rome at the Institute of Clinical Physiology (National Research Council of Italy) (IFC-CNR) [22][33].

CARDIOSIM[®] is a numerical simulator of the cardiovascular system based on lumped parameter models, modified time-varying elastance and pressure-volume analysis of ventricular function. The software is interactive and can reproduce physiological and pathological conditions for clinical decision-making in a controlled environment [23][24]. The main feature is a modular approach with an updatable library of numerical models of different sections of the cardiovascular system, which can be assembled according to the need of the simulation. The software is particularly suitable to study the interactions with pulsatile or continuous flow ventricular assist devices [19][20][21][24], intra-aortic balloon pump, artificial lung, biventricular assist device and biventricular pacing [16][17][18][24][25].

CHAPTER 2: AIM OF THE STUDY

The aim of this thesis is the use of a simulation approach for the optimization of device-based treatment and to guide therapeutic intervention in advanced heart failure. Preliminary studies from this group have already shown the feasibility of this approach [11][12].

CHAPTER 3: MATERIALS AND METHODS

A retrospective analysis of hemodynamic data measured in six heart failure patients from the Scottish National Advanced Heart Failure Service, Glasgow, UK was undertaken to reproduce their preoperative hemodynamic status and then carry out simulations in the presence of a ventricular assist device in order to evaluate their suitability for prolonged mechanical support or other intervention. The aim was to compare the outcome of the simulations with the previously made clinical decisions in order to find out any relationship that may be applicable on a routine basis in future patient assessment. This would lead to a more targeted approach for specific group of patients, more quantitative evaluation in the clinical decision process, and optimization of preoperative planning and treatment, with the added predictive value of simulation [11][12].

The thesis was developed at the Institute of Clinical Physiology IFC-CNR, in the Cardiovascular Numerical/Hybrid Modelling Lab of Rome. The study was carried out using a numerical simulator of the cardiovascular system, CARDIOSIM[®], which enables to reproduce patho-physiological conditions. Different mechanical circulatory support systems (MCSS) have been implemented in the simulator in order to study the interaction between assist devices and the cardiovascular system in terms of hemodynamic and ventricular energetic parameters [24]. To describe the different circulatory compartments a lumped parameter model [35] was used, while the ventricular, atrial and septal components were implemented using a variable elastance model [82].

3.1 A Lumped-parameter Model of the Cardiovascular System

The cardiovascular system can be considered as a large closed-loop hydraulic network driven by a pulsatile pump [69][78], where a different behaviour is observed according to the location in the system. For example, wave propagation in the arterial tree is of greater influence whereas it is almost steady in the capillary bed highlighting the lumped features of the system. On the other hand, local phenomena like branching create flow perturbations showing the interdependence of different scales of the system and the need of a multi-compartment approach [69]. The windkessel model is a simplified but effective description of the cardiovascular compartments [51][68][69]. First developed by Frank in 1899, the windkessel is a lumped parameter model derived from electrical circuit analogies where the current represents arterial blood flow and voltage represents arterial pressure. Resistances represent arterial and peripheral resistance that occur as a result of viscous dissipation inside the vessels, capacitors represent volume compliance of the vessels that allows them to store large amounts of blood, and inductors represent inertia of the blood [51]. These models consider a uniform distribution of fundamental variables (pressure, volume and flow rate) in every single compartment (organ, blood vessel, etc.) as a function of time; the spatial distribution of the parameters can be approximated by setting up multi-compartment, each of them considered homogeneous and represented by a different lumped parameter model [68]. The main advantage of these models is that they rely on ordinary differential equations, which are easy to understand and solve although it is not obvious how to estimate their parameters from measurements of arterial blood flow and pressure [51].

The different circulatory compartments are represented in CARDIOSIM[®] using a lumped parameter model [24]. The software has a modular structure with different sections: left/right atrium and ventricle, pulmonary venous/arterial system, systemic venous/arterial system, coronary circulation (Fig. 3).

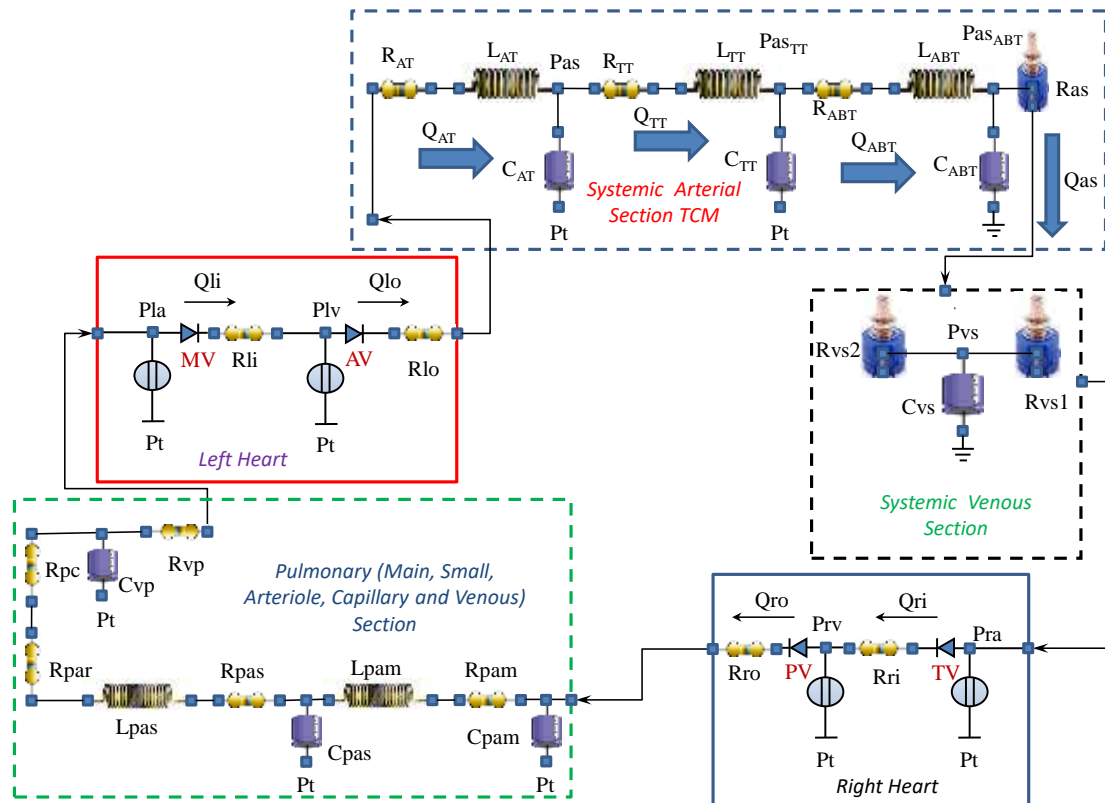
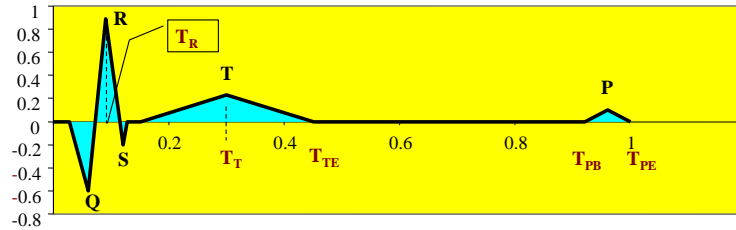


Fig. 3 Electrical analogue of the cardiovascular system used in order to perform our simulations

As shown in Fig. 3, the systemic arterial section consists of three RLC elements representing the aortic (R_{AT} , L_{AT} and C_{AT}), thoracic (R_{TT} , L_{TT} and C_{TT}) and abdominal (R_{ABT} , L_{ABT} and C_{ABT}) tract respectively. R_{as} is the variable systemic peripheral resistance. The main (small) pulmonary section is reproduced by a RLC element: R_{pam} , L_{pam} and C_{pam} (R_{pas} , L_{pas} and C_{pas}). The arteriole (capillary) bed behaviour is reproduced by a single resistance R_{par} (R_{pc}). The pulmonary venous section consists of a compliance (C_{vp}) and a resistance (R_{vp}). P_t is the mean intrathoracic pressure. The systemic venous section is modelled with the compliance C_{vs} and the two resistances R_{vs1} and R_{vs2} . In the left and right heart sections, each valve is modelled as a diode with a resistance, assuming a unidirectional blood flow. R_{li} and R_{lo} represent the resistances of the mitral and aortic valves respectively (MV and AV); R_{ri} and R_{ro} are the resistances of the pulmonary and tricuspid valves (PV and TV).

3.2 Ventricular and Atrial Numerical Modelling

A variable elastance model is used to describe atrial and ventricular behaviour in CARDIOSIM[®], while their mechanical properties are related to the ECG signal [24] (Fig. 4).



T_R	R wave peak time
T_T	T wave peak time [Ventricular ejection starting]
T_{TE}	Ventricular systole ending
$T_T - T_{TE}$	Ventricular systole duration
T_{PB}	Atrial depolarization starting
T_{PE}	Atrial depolarization ending
$T_{PE} - T_{PB}$	Atrial depolarization duration

Fig. 4 Schematic representation of the ECG signal

The following equations are used to reproduce the behaviour of the instantaneous left/right ventricular pressure ($Plv(t)/Prv(t)$):

$$\begin{cases} Plv(t) = \frac{e_{ventrSPT}(t) \cdot elv(t)}{e_{ventrSPT}(t) + elv(t)} \cdot (Vlv(t) - V_0lv) + \frac{elv(t)}{e_{ventrSPT}(t) + elv(t)} \cdot Prv(t) \\ Prv(t) = \frac{e_{ventrSPT}(t) \cdot erv(t)}{e_{ventrSPT}(t) + erv(t)} \cdot (Vrv(t) - V_0rv) - \frac{erv(t)}{e_{ventrSPT}(t) + erv(t)} \cdot Plv(t) \end{cases} \quad (1)$$

$Vlv(t)$ and $Vrv(t)$ are the instantaneous left and right ventricular volumes. V_0lv (V_0rv) is the left (right) rest ventricular volume.

$elv(t)$ and $erv(t)$ are the left and right ventricular time-varying elastance and are expressed by:

$$elv(t) = Elvd + \frac{Elvs - Elvd}{2} alv(t) \quad erv(t) = Ervd + \frac{Ervs - Ervd}{2} arv(t) \quad (2)$$

$Elvs$ and $Ervs$ are the left and right ventricular systolic elastances. $Elvd$ and $Ervd$ are the left and right ventricular diastolic elastances.

$alv(t)/arv(t)$ is the left/right activation function describing the contraction and the relaxation phases of the ventricles and can be written as follows:

$$alv(t) = arv(t) = \begin{cases} 1 - \cos\left(\frac{t}{T_T} \pi\right) & 0 \leq t \leq T_T \\ 1 + \cos\left(\frac{t - T_T}{T_{TE} - T_T} \pi\right) & T_T < t \leq T_{TE} \\ 0 & T_{TE} < t \leq T \end{cases} \quad (3)$$

where T_{TE} is the end of ventricular systole and T_T is the T-wave peak time, as shown in Fig. 4. In Eq. 1, $e_{ventrSPT}(t)$ is the interventricular septum systolic elastance, which corresponds to:

$$e_{ventrSPT}(t) = Ed_{ventrSPT} + \frac{Es_{ventrSPT} - Ed_{ventrSPT}}{2} a_{ventrSPT}(t) \quad (4)$$

where $a_{ventrSPT}(t)$ is the activation function described as follows:

$$a_{ventrSPT}(t) = \begin{cases} 1 - \cos\left(\frac{t}{T_R} \pi\right) & 0 \leq t \leq T_R \\ 1 + \cos\left(\frac{t - T_R}{T_{TE} - T_R} \pi\right) & T_R < t \leq T_{TE} \\ 0 & T_{TE} < t \leq T \end{cases} \quad (5)$$

T_{TE} is still the end of ventricular systole and T_R is the R-wave peak time (Fig. 4).

The same variable elastance model is also used to describe the behaviour of the left and right atria, with the following equation representing the instantaneous left/right atrial pressure ($Pla(t)/Pra(t)$):

$$\begin{cases} Pla(t) = \frac{e_{atriaSPT}(t) \cdot ela(t)}{e_{atriaSPT}(t) + ela(t)} \cdot (Vla(t) - V_0la) + \frac{ela(t)}{e_{atriaSPT}(t) + ela(t)} \cdot Pra(t) + \frac{e_{atriaSPT}(t)}{e_{atriaSPT}(t) + ela(t)} \cdot P_0la \\ Pra(t) = \frac{e_{atriaSPT}(t) \cdot era(t)}{e_{atriaSPT}(t) + era(t)} \cdot (Vra(t) - V_0ra) + \frac{era(t)}{e_{atriaSPT}(t) + era(t)} \cdot Pla(t) + \frac{e_{atriaSPT}(t)}{e_{atriaSPT}(t) + era(t)} \cdot P_0ra \end{cases} \quad (6)$$

$Vla(t)$ and $Vra(t)$ are the instantaneous left and right atrial volumes. V_0la (V_0ra) is the left (right) rest atrial volume.

$ela(t)$ and $era(t)$ are the left and right atrial time-varying elastance and are expressed by:

$$ela(t) = Elad + \frac{Elas - Elad}{2} ala(t) \quad era(t) = Erad + \frac{Eras - Erad}{2} ara(t) \quad (7)$$

E_{las} and E_{ras} are the left and right atrial systolic elastances. E_{lad} and E_{rad} are the left and right atrial diastolic elastances.

$ala(t)/ara(t)$ is the left/right atrial activation function that can be written as follows:

$$ala(t) = ara(t) = \begin{cases} 0 & 0 \leq t \leq T_{PB} \\ 1 + \cos\left(\frac{t - T_{PB}}{T_{PE} - T_{PB}} 2\pi\right) & T_{PB} < t \leq T_{PE} \\ 0 & T_{PE} < t \leq T \end{cases} \quad (8)$$

where T_{PB} is the start of atrial depolarization (P wave) and T_{PE} is the end of it (Fig. 4).

In Eq. 6, $e_{atriaSPT}(t)$ is the interatrial septum systolic elastance, which corresponds to:

$$e_{atriaSPT}(t) = Ed_{atriaSPT} + \frac{Es_{atriaSPT} - Ed_{atriaSPT}}{2} a_{atriaSPT}(t) \quad (9)$$

where $a_{atriaSPT}(t)$ is the activation function described as follows:

$$a_{atriaSPT}(t) = \begin{cases} 0 & 0 \leq t \leq T_{PB} \\ 1 + \cos\left(\frac{t - T_{PB}}{T_{PE} - T_{PB}} 2\pi\right) & T_{PB} < t \leq T_{PE} \\ 0 & T_{PE} < t \leq T \end{cases} \quad (10)$$

T_{PB} and T_{PE} still representing the onset and the end of the P wave of the ECG signal.

3.3 Berlin Heart INCOR® Pump

The Berlin Heart INCOR® Pump is the LVAD integrated in the software and used for our simulations (Fig. 5).



Fig. 5 Berlin Heart INCOR® Pump

The INCOR® System is a unique pump specifically designed for long-term support (Destination Therapy) although it can be implanted as Bridge to Transplant and Bridge to

Recovery. The blood coming from the left ventricle flows into the device through the inlet guide vane, which ensures laminar inflow to the rotor. An active magnetic bearing enables the rotor to float contact-free and produce the required pumping work at 5,000 to 10,000 rpm. The outlet guide vane behind the rotor generates additional pressure with a specially aligned blade and directs the blood in the outlet cannula to the aorta. The necessary electrical energy to drive the pump is supplied by a cable tunneled through the skin on the right side of the patient. The pump cable is connected to the driving unit via a plug connector close to the patient. The driving unit is battery powered and controls the entire system (Fig. 6).



Fig. 6 Berlin Heart INCOR[®] Pump. Battery, driving unit and bag

The INCOR[®] pump creates a constant blood flow which, in combination with the native left ventricle, leads to pulsatility in the patient.

The Individual Components of the device are the following:

- Inflow cannula
- Axial pump
- Main battery
- Control unit
- Plug connector
- Backup battery
- Pump cable
- Outflow angle (n/a with lateral access)
- Outflow cannula

Occasionally active components are:

- Mains power supply unit
- Charging unit
- Laptop with monitoring program

A specially designed bag enables safe keeping and transport of the components.
An electric analogue of the device model is shown in Fig. 7.

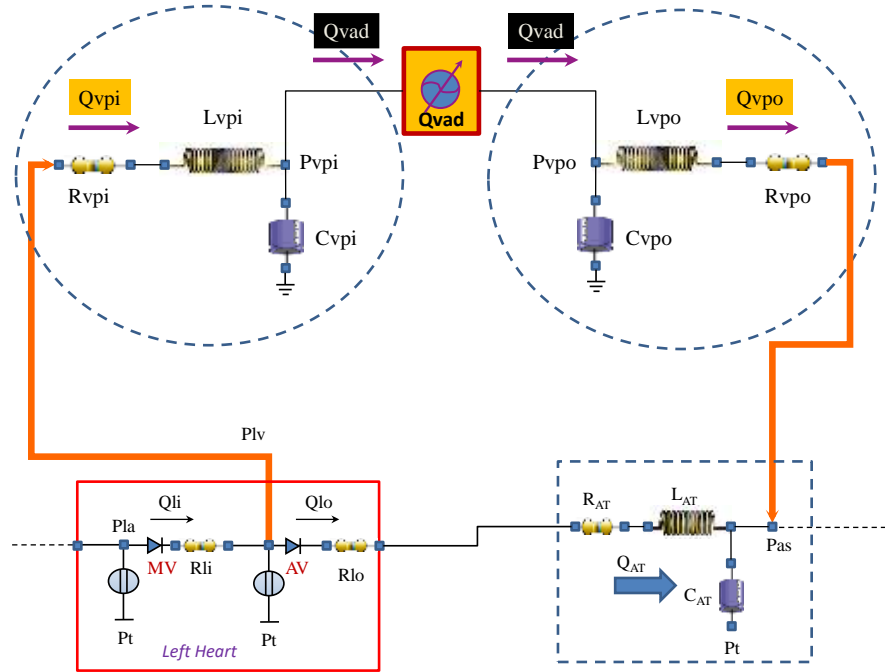


Fig. 7 Electrical analogue of Berlin Heart INCOR® Pump

P_{lv} ad P_{as} are the left ventricular and systemic arterial pressures respectively. The Input and output pump cannulae are modelled with a resistance R_{vpi} and R_{vpo} , a compliance C_{vpi} and C_{vpo} , an inductance L_{vpi} and L_{vpo} ; Q_{vad} is the pump flow; Q_{vpi} and Q_{vpo} are the input and output cannulae flow.

Setting parameters are shown in Table 3.

Table 3 Setting parameters of the Berlin Heart INCOR® Pump

Inlet and outlet cannulae parameters		
Parameter	Value	Unit
C_{vpi} [C_{vpo}]	0.1 [0.1]	mmHg ⁻¹ ·ml
R_{vpi} [R_{vpo}]	0.01 [0.01]	mmHg·s·ml ⁻¹
L_{vpi} [L_{vpo}]	$1.2 \cdot 10^{-4}$ [$1.2 \cdot 10^{-4}$]	mmHg·s ² ·ml ⁻¹
LVAD parameter		
Pump speed	6000; 8900; 10000	Rpm
$K_{vad,0}$	90.5184	L·min ⁻¹
$K_{vad,1}$	$-3.0361 \cdot 10^{-3}$	L·min ⁻¹ ·rpm ⁻¹
$K_{vad,2}$	-1.23045	L·min ⁻¹ ·mmHg ⁻¹
$K_{vad,3}$	$5.78974 \cdot 10^{-4}$	L·min ⁻¹ ·rpm ⁻¹ ·mmHg ⁻¹
$K_{vad,4}$	$-5.8777 \cdot 10^{-8}$	L·min ⁻¹ ·rpm ⁻² ·mmHg ⁻¹
$K_{vad,5}$	$-1.27359 \cdot 10^{-6}$	L·min ⁻¹ ·rpm ⁻¹ ·mmHg ⁻²
$K_{vad,6}$	$2.04834 \cdot 10^{-10}$	L·min ⁻¹ ·rpm ⁻² ·mmHg ⁻²

The inlet and outlet cannulae flows are calculated as follows:

$$\left\{ \begin{array}{l} (P_{lv} + P_t) - P_{vpi} = Q_{vpi} \cdot R_{vpi} + L_{vpi} \frac{dQ_{vpi}}{dt} \\ Q_{vpi} = Q_{vad} + C_{vpi} \frac{dP_{vpi}}{dt} \end{array} \right. \quad \left\{ \begin{array}{l} P_{vpo} - (P_{as} + P_t) = Q_{vpo} \cdot R_{vpo} + L_{vpo} \frac{dQ_{vpo}}{dt} \\ Q_{vpo} = Q_{vad} - C_{vpo} \frac{dP_{vpo}}{dt} \end{array} \right. \quad (11)$$

where P_{vpi} and P_{vpo} are the inlet and outlet cannulae pressures. P_t is the mean intrathoracic pressure.

The flow produced by the LVAD is described by:

$$Q_{vad} = K_{vad,0} + \omega \cdot K_{vad,1} + K_{vad,2} \cdot (P_{vpo} - P_{vpi}) + K_{vad,3} \cdot \omega \cdot (P_{vpo} - P_{vpi}) + \quad (12)$$

$$+ K_{vad,4} \cdot \omega^2 \cdot (P_{vpo} - P_{vpi}) + K_{vad,5} \cdot \omega \cdot (P_{vpo} - P_{vpi})^2 + K_{vad,6} \cdot \omega^2 \cdot (P_{vpo} - P_{vpi})^2$$

where:

$$\omega(t) = A_0 + A_p \cdot \sin\left(\frac{2\pi t}{T} + \varepsilon_0\right) \quad (13)$$

A_0 is the component of the LVAD speed, A_p is the amplitude of the pulsation component, ϵ_0 is the phase difference between the LVAD pulsation component and the native cardiac timing.

3.4 Patient Analysis and Simulations

We investigated the value of simulation in the context of six heart failure patients previously discussed at a multidisciplinary meeting and treated accordingly, with a view to predict or guide future management.

In order to reproduce the starting measured conditions of each patient, after manual insertion of HR (Heart Rate), BP (mean Blood Pressure), SV (Stroke Volume), LVEF (Left Ventricular Ejection Fraction) and BSA (Body Surface Area) the CARDIOSIM[®] software estimates both end-diastolic volume (EDV) and end-systolic volume (ESV) and also the left ventricular end-systolic pressure volume relationship (ESPVR) slope (Ees) in order to position the left ventricular loop in the Pressure - Volume (PV) plane (Fig.8).

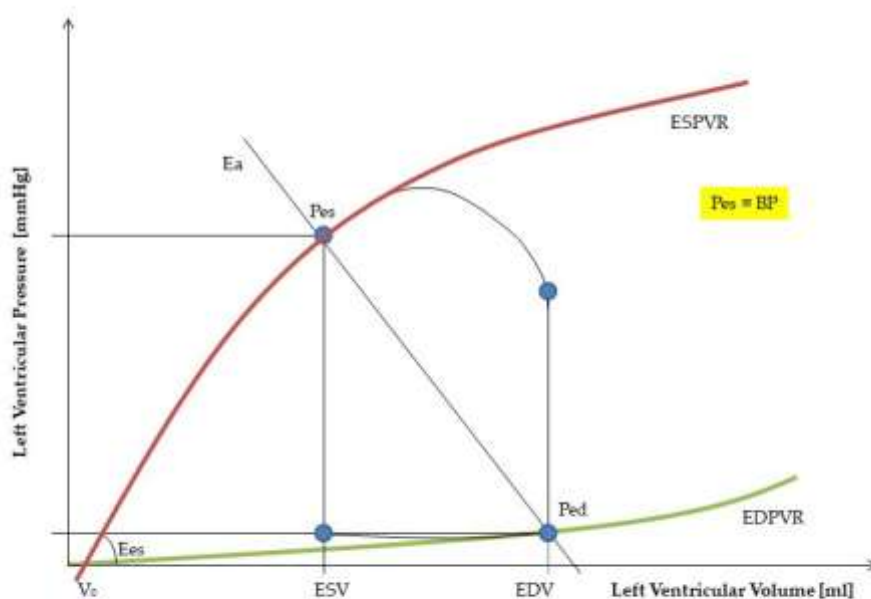


Fig. 8 Left Ventricular Loop in the PV plane

The BP value (that approximates the end-systolic pressure, P_{es}) allows the software to estimate the Ees slope through the P_{es} -Stroke Volume (SV) relationship and at the same time, it allows to determine the left ventricular end-systolic volume (ESV). The simulated P_{la} value (left atrial pressure \equiv PCWP, pulmonary capillary wedge pressure) allows the software to reproduce the left ventricular filling together with the end-diastolic volume (EDV).

The retrospective analysis was performed starting by hemodynamic data of the following patients:

3.4.1 Patient #1

A 34-year-old patient who sustained an extensive anterior wall myocardial infarction treated initially with a Percutaneous coronary intervention (PCI) procedure and the insertion of a drug-eluting stent to the Left Anterior Descending (LAD) coronary artery. Afterwards, stent occlusion and residual LV systolic dysfunction (LVEF of 27%) required full anti-failure treatment. With subsequent deterioration and worsening of the clinical picture, dobutamine infusion and close monitoring were needed. The presence of co-morbidities, particularly a high BMI, made this patient unsuitable for transplantation while the insertion of a LVAD was considered unlikely to be beneficial. Hemodynamic data from right heart catheterisation (RHC) showed persistently elevated Pulmonary Arterial Pressures and resistance with reduced right ventricular stroke work index; these data would have increased the need for right ventricular support following LVAD insertion with potential for prolonged intensive care need and increased risks. A multidisciplinary team (MDT) meeting decided to go on with medical management and palliative care.

Table 4 shows hemodynamic data on admission and 4 days later. The values in black are measured data; those in blue are estimated data calculated during the studies carried out for this thesis.

Table 4 Hemodynamic data of Patient #1 on Admission and after 4 days

Patient #1	Legend	RHC 1 (Admission)			RHC 2 (After 4 days)		
		Max	Min	Mean	Max	Min	Mean
BP [mmHg]	Blood Pressure	85/90	59	69.3	85/90	60	70
RA [mmHg]	Right Atrial Pressure	35	17	29	38	22	32
RV [mmHg]	Right Ventricular Pressure	61	14	38	71	11	44
PA [mmHg]	Pulmonary Arterial Pressure	62	30	42	70	38	50
PCWP [mmHg]	Pulmonary Capillary Wedge Pressure	36	31	32	35	25	34
TPG [mmHg]	Transpulmonary Pressure Gradient TPG=PA-PCWP	10			16		
CO [L/min]	Cardiac Output CO=HR*SV	2.7			2.8		
CI [L/min/m²]	Cardiac Index CI= CO/BSA	1.36			1.4		
PVR [wood unit]	Pulmonary Vascular Resistance	3.7			5.7		
RVSWI [g/m²/beat]	Right Ventricular Stroke Work Index RVSWI= (PA-RA)*SVI*0.0136	2.4			2.4		
HR [bpm]	Heart Rate HR = CO/SV	100			95		
BSA [m²]	Body Surface Area	1.98			1.98		
LVEF	Left Ventricular Ejection Fraction LVEF = SV/EDV = (EDV-ESV)/EDV	27%			27%		
Estimated values							
EDV [ml]	End Diastolic Volume EDV ≈ (CO/HR)/LVEF%	~100			~109		
ESV [ml]	End systolic Volume ESV = EDV - SV	~73			~80		
Ea [mmHg/ml]	Arterial Elastance Ea ≈ BP/SV	~3.0			~2.8		

3.4.2 Patient #2

A 55-year-old patient who previously underwent aortic valve replacement with a mechanical prosthesis and subsequently developed critical LAD stenosis treated with PCI. His background consisted of hypertrophic cardiomyopathy with LVEF of 45%, in the context of chronic atrial fibrillation, previous ventricular arrhythmias and renal impairment. Further deterioration and worsening of symptoms led to multiple hospital admissions, adjustment of

anti-failure therapy and the start of Milrinone (PDE3 inhibitor) infusion. Following a MDT, the patient was considered unsuitable for LVAD insertion and listed for transplant.

Table 5 shows hemodynamic data on admission and after one and two months.

Table 5 Hemodynamic data of Patient #2 on Admission and after 1 and 2 months

Patient #2	RHC 1 (Admission)			RHC 2 (After 1 month)			RHC 3 (After 2 months)		
	Max	Min	Mean	Max	Min	Mean	Max	Min	Mean
BP [mmHg]	95/100	58	72	-	-	-	-	-	-
RA [mmHg]	14	2	9	10	4	6	11	1	7
RV [mmHg]	39	2	17	37	1	15	32	-2	14
PA [mmHg]	40	17	27	34	15	26	31	14	22
PCWP [mmHg]	28	7	18	26	8	15	26	11	15
TPG [mmHg]	9			11			7		
CO [L/min]	5.3			7.1			5.6		
CI [L/min/m ²]	2.26			3.02			2.4		
PVR [wood unit]	1.7			1.55			1.25		
RVSWI [g/m ² /beat]	8.5			9.35			6.2		
HR [bpm]	65			88			78		
BSA [m ²]	2.35			2.35			2.35		
LVEF	45%			-			-		
Estimated values									
EDV [ml]	~181			-			-		
ESV [ml]	~99			-			-		
Ea [mmHg/ml]	~1.1			-			-		

3.4.3 Patient #3

A 52-year-old patient with a previous myocardial infarction requiring bypass grafting and subsequent implantable cardioverter-defibrillator (ICD) insertion to avoid potentially fatal ventricular arrhythmias. Worsening of his clinical conditions required multiple hospital admissions in a context of left ventricular dilation (LV end-diastolic diameter 8.1 cm) with severe systolic and diastolic dysfunction (LVEF 15%) and severe pulmonary hypertension. Further deterioration required Milrinone and diuretics infusion with the insertion of an intra-aortic balloon pump. After a MDT meeting, the patient was placed on the transplant list with a view to LVAD insertion in case of further deterioration.

Table 6 shows hemodynamic data on admission and after 15 and 22 days.

Table 6 Hemodynamic data of Patient #3 on Admission and after 15 and 22 days

Patient #3	RHC 1 (Admission)			RHC 2 (After 15 days)			RHC 3 (After 22 days)		
	Max	Min	Mean	Max	Min	Mean	Max	Min	Mean
BP [mmHg]	100	60	73.3	-	-	-	-	-	-
RA [mmHg]	14	12	9	18	11	15	14	6	10
RV [mmHg]	53	5	-	60	4	28	67	-3	28
PA [mmHg]	58	27	37	75	33	44	75	36	48
PCWP [mmHg]	39	29	31	48	26	35	47	26	33
TPG [mmHg]	6			9			15		
CO [L/min]	4.2			4.5			2.6		
CI [L/min/m ²]	1.94			2.1			1.2		
PVR [wood unit]	1.4			2			6.8		
RVSWI [g/m ² /beat]	9.87			11.4			9.15		
HR [bpm]	75			72			68		
BSA [m ²]	2.16			2.16			2.16		
LVEF	15%			-			-		
Estimated values									
EDV [ml]	~373			-			-		
ESV [ml]	~317			-			-		
Ea [mmHg/ml]	~1.6			-			-		

3.4.4 Patients #4, #5 and #6.

Less data were provided for the last three patients.

Patient #4 is 29 years old with dilated cardiomyopathy; Patient #5 is 58 years old with ischaemic cardiomyopathy; Patient #6 is 51 years old with ischaemic cardiomyopathy. All of them required multiple hospital admissions with deterioration of symptoms despite the highest medical treatment. LVAD support was required for all of them and Patient #4 underwent cardiac transplantation after 12 months of mechanical circulatory support.

Table 7 shows baseline admission parameters.

Table 7 Hemodynamic data of Patients #4, #5 and #6 on Admission

	Patient #4 [RHC 1]			Patient #5 [RHC 1]			Patient #6 [RHC 1]		
	Max	Min	Mean	Max	Min	Mean	Max	Min	Mean
BP [mmHg]	85	69.6	59	112	68	82	106	70	82
RA [mmHg]	-	-	8	-	-	12	-	-	14
RV [mmHg]	60	9	30	71	23	39	57	10	23
PA [mmHg]	64	34	49	67	27	43	68	41	53
PCWP [mmHg]	-	-	39	41	20	30	-	-	49
TPG [mmHg]	10			11			4		
CO [L/min]	4.6			5.4			3.2		
CI [L/min/m²]	2.51			2.87			1.6		
PVR [wood unit]	2.17			2.04			1.25		
RVSWI [g/m²/beat]	17.97			15.14			8.16		
HR [bpm]	78			80			102		
BSA [m²]	1.83			1.88			2.02		
LVEF	21%			36%			21%		
Estimated values									
EDV [ml]	~280.8			~187.5			~149.4		
ESV [ml]	~221.8			~120			~118		
Ea [mmHg/ml]	~1.3			~1.49			~3.04		

CHAPTER 4: RESULTS**4.1 Patient #1**

The simulations with LVAD assistance for the first three patients were performed with a pump speed of 6000 rpm, which gave the best results.

Table 8 shows the measured parameters and simulation results obtained for Patient #1.

Table 8 Measured parameters and simulation results for Patient #1

Patient #1	Measured [RHC 1]			Simulation [RHC 1]			LVAD (Simulation)		
	Max	Min	Mean	Max	Min	Mean	Max	Min	Mean
BP [mmHg]	85-90	59	69.3	87.2	60.7	69.3	75.2	62.9	68.2
RA [mmHg]	35	17	29	10.5	3.5	6.5	10.3	3.5	6.5
RV [mmHg]	61	14	38	44.2	8.0	20.4	43.5	8.0	20.1
PA [mmHg]	62.0	30.0	42.0	44.0	39.7	42.0	43.3	38.7	40.9
PCWP [mmHg]	36.0	21.0	32.0	31	18.7	25.0	29.6	16.8	23.1
HR [bpm]	100			100			100		
LVEF	27%			26.9%			31.4%		
BSA [m ²]	1.98			1.98			1.98		
CO [L/min]	2.7			2.7			CO _{VENTR}	0.67	
							Q _{VAD}	2.15	
							TOT	2.82	
CI [L/min/m ²]	1.36			1.36			0.34		
TPG [mmHg]	10			17			18		
PVR [wood unit]	3.7			6.3			26.87 (18.0/0.67)		
							6.38 (18.0/2.15)		
RVSWI [g/m ² /beat]	2.4			6.53			6.86		
	Estimated			Simulated			Simulated		
EDV [ml]	~100			100.4			89.76		
ESV [ml]	~73			73.4			61.57		
Ea [mmHg/ml]	~3.0			3.2			2.6		
Ees[mmHg/ml]	-			0.88			0.88		
Ea/Ees	-			3.64			2.95		

The clinical parameters measured on hospital admission (baseline) have been listed in the second column. Minimum, maximum and mean pressure values were measured. EDV, ESV and Ea were calculated starting from measured LVEF, HR and mean BP. The third column shows the baseline parameters reproduced by the numerical simulator. Ea, the slope Ees of the ESPVR and the Ea/Ees ratio were calculated by CARDIOSIM[®]. The Ea/Ees ratio represents a reliable index of ventricular–arterial coupling in normal conditions. The

simulated parameters during LVAD assistance have been listed in the fourth column. CO after the simulation consists of three values: the total cardiac output (Q_{TOT}), the left ventricular output flow (CO_{VENTR}) and the LVAD output flow (Q_{VAD}). PVR consists of two different values: the first one is calculated as the ratio between TPG and CO_{VENTR} , the second one is calculated as the ratio between TPG and Q_{VAD} .

4.2 Patient #2

Table 9 shows the measured parameters and simulation results for Patient #2.

Table 9 Measured parameters and simulation results for Patient #2

Patient #2	Measured [RHC 1]			Simulation [RHC 1]			LVAD (Simulation)			LVAD Milrinone(10%) (Simulation) +		
	Max	Min	Mean	Max	Min	Mean	Max	Min	Mean	Max	Min	Mean
BP [mmHg]	95-100	58	72	97.2	60.5	72	81.7	63.3	70.6	82.2	62.6	70.5
RA [mmHg]	14.0	2.0	9.0	14.9	5.4	10.0	14.9	5.5	10.0	15.2	5.3	10.1
RV [mmHg]	39.0	2.0	17.0	33.5	5.0	14.8	33.6	5.4	15.9	33.4	3.7	14.9
PA [mmHg]	40.0	17.0	27.0	33.0	14.4	23.2	32.2	13.3	22.5	32.9	12.7	22.6
PCWP [mmHg]	28.0	7.0	18.0	26.6	8.9	14.3	25.9	7.9	13.4	27.3	7.6	13.6
HR [bpm]	65			65			65			65		
LVEF	45%			45.1%			49.8%			55.9%		
BSA [m ²]	2.35			2.35			2.35			2.35		
CO [L/min]	5.3			5.3			CO_{VENTR}	1.72		CO_{VENTR}	2.04	
							Q_{VAD}	3.67		Q_{VAD}	3.92	
							Q_{TOT}	5.39		Q_{TOT}	5.96	
CI [L/min/m ²]	2.26			2.26			0.73			0.82		
TPG [mmHg]	9			8.9			9.1			9.0		
PVR [wood unit]	1.7			1.68			5.3 (9.1/1.72)			4.41 (9.0/2.04)		
							2.48 (9.1/3.67)			2.30 (9.0/3.92)		
RVSWI [g/m ² /beat]	8.5			6.23			6.0			6.63		
	Estimated			Simulated			Simulated			Simulated		
EDV [ml]	~181			180.74			166.4			163.83		
ESV [ml]	~99.6			99.2			83.5			72.2		
Ea [mmHg/ml]	~1.1			1.1			0.9			0.9		
Ees[mmHg/ml]	-			0.68			0.68			0.748		
Ea/Ees	-			1.62			1.32			1.2		

The baseline and simulated parameters have been listed in the second and third columns. The parameters obtained during LVAD support and LVAD support with Milrinone administration

have been listed in the fourth and fifth columns. The phosphodiesterase 3 inhibitor increases myocardial contractility and reduces peripheral resistances by $\approx 10\%$ from baseline values according to literature data [40].

Fig. 9 shows a screen output produced by our simulator for Patient #2.

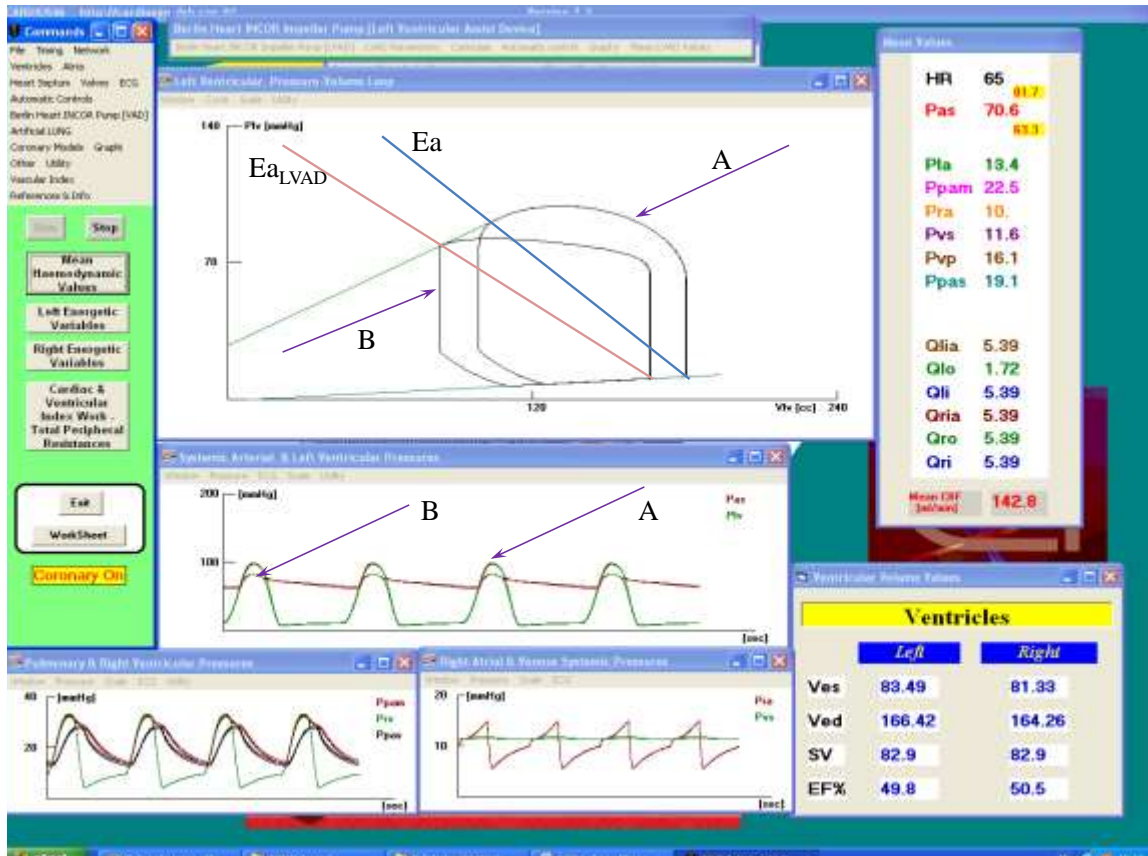


Fig. 9 Screen output obtained from **CARDIOSIM**[®] showing “Admission” (PV loop A) and assisted (PV loop B) conditions for Patient #2

The upper window in Fig. 9 shows the pressure – volume (PV) loop of the simulated admission conditions (A) and the PV loop after LVAD support (B). ESPVR and EDPVR are also plotted (green lines). A reduction in the slope of the arterial elastance Ea_{LVAD} is observed during LVAD support. The mean values for pressure, flow and HR have been listed in the right upper box and calculated during the cardiac cycle in the presence of LVAD assistance. Pas represents the mean arterial pressure ($Pas \equiv BP$), with systolic and diastolic values reported above and below it; Pla is the mean left atrial pressure ($Pla \equiv PCWP$); Pra is the mean right atrial pressure; $Ppam$ is the mean pulmonary arterial pressure ($Ppam \equiv PA$), Pvs is the systemic venous pressure, and Pvp is the pulmonary venous pressure. The mean left/right atrial input flow ($Qlia/Qria$), left/right ventricular input flow (Qli/Qri) and right ventricular output flow (Qro) have the same value; the sum of the mean left ventricular output flow (Qlo) and the LVAD flow ($Qvad$) equals the flow into the circulatory network ($Qlo + Qvad = Qlia = Qria = Qro = Qri = Qli$). CBF is the coronary blood flow. The central

window shows the instantaneous waveform representing the mean Pas in conditions (A) and (B). Finally, the right lower box shows the end-systolic volume ($V_{es} \equiv ESV$), the end-diastolic volume ($V_{ed} \equiv EDV$), the SV and the EF for both ventricles.

4.3 Patient #3

Table 10 shows the measured parameters and simulation results obtained for Patient #3.

Table 10 Measured parameters and simulation results for Patient #3

Patient #3	Measured [RHC 1]			Simulation [RHC 1]			LVAD (Simulation)			LVAD Milrinone (10%) (Simulation) +		
	Max	Min	Mean	Max	Min	Mean	Max	Min	Mean	Max	Min	Mean
BP [mmHg]	100	60	73.3	106.7	60	73.4	82.8	66.6	74.1	85.2	67.4	74.6
RA [mmHg]	14	12	9.0	8.8	1.7	4.4	9.0	1.7	4.6	9.2	0.5	4.6
RV [mmHg]	53	5.0	-	33.0	1.0	11.6	31.5	1.0	11.3	32.4	0.5	11.6
PA [mmHg]	58.0	27.0	37.0	32.8	22.6	28.0	31.3	20.4	26.2	32.2	19.9	26.5
PCWP [mmHg]	39.0	29.0	31.0	28.4	12.3	18.0	26.8	9.5	15.4	28.0	8.9	15.5
HR [bpm]	75			75			75			75		
LVEF	15%			15%			18.9%			21.9%		
BSA [m ²]	2.16			2.16			2.16			2.16		
CO [L/min]	4.2			4.2			CO _{VENTR}	0.74		CO _{VENTR}	0.93	
							Q _{VAD}	3.8		Q _{VAD}	4.22	
							Q _{TOT}	4.54		Q _{TOT}	5.15	
CI [L/min/m ²]	1.94			1.94			0.34			0.43		
TPG [mmHg]	6			10.0			10.8			11		
PVR [wood unit]	1.43			2.38			14.6 (10.8/0.74)			11.83 (11/0.93)		
							2.84 (10.8/3.8)			2.61 (11/4.22)		
RVSWI [g/m ² /beat]	9.87			8.32			8.23			9.47		
	Estimated			Simulated			Simulated			Simulated		
EDV [ml]	~373			372.53			320.16			313.74		
ESV [ml]	~317			316.55			259.6			245.0		
Ea [mmHg/ml]	~1.6			1.9			1.3			1.2		
Ees[mmHg/ml]	-			0.4			0.4			0.44		
Ea/Ees	-			4.75			3.25			2.73		

Again, measured and simulated parameters on admission are shown in the second and third columns. The results obtained during simulated LVAD assistance alone and with Milrinone are shown in the fourth and fifth columns

4.4 Patient #4

Tables 11 and 12 show the measured parameters and simulation results obtained for Patient #4. The effect of LVAD support at different pump speed (8900 rpm and 6000 rpm) was considered for comparison in view of the patho-physiological background.

Table 11 Measured parameters and simulation results for Patient #4

Patient #4	Measured [RHC 1]			Simulation [RHC 1]			LVAD [8900 rpm] (Simulation)		
	Max	Min	Mean	Max	Min	Mean	Max	Min	Mean
BP [mmHg]	85	62	69.6	87.2	60.7	69.3	80.6	68.0	71.0
RA [mmHg]	-	-	8.0	-	-	3.6	-	-	3.5
RV [mmHg]	60	9.0	30	65	1.0	19	61.4	1.0	18.0
PA [mmHg]	64	34.0	49.0	-	-	55.4	-	-	50
PCWP [mmHg]	-	-	39.0	-	-	37	-	-	31.6
HR [bpm]	78			78			78		
LVEF	21%			21%			15.1%		
BSA [m ²]	1.83			1.83			1.83		
CO [L/min]	4.6			4.6			CO _{VENTR}		1.13
							Q _{VAD}		3.82
							Q _{TOT}		4.95
CI [L/min/m ²]	2.51			2.51			0.62		
TPG [mmHg]	10			18.4			18.4		
PVR [wood unit]	2.17			4.0			16.28 (18.4/1.13)		
							4.82 (18.4/3.82)		
RVSWI [g/m ² /beat]	17.97			22.7			21.93		
	Estimated			Simulated			Simulated		
EDV [ml]	~280.8			280.7			233.7		
ESV [ml]	~221.8			221.7			198.4		
Ea [mmHg/ml]	~1.3			1.6			2.3		
Ees[mmHg/ml]	-			0.468			0.468		
Ea/Ees	-			3.42			4.91		

The measured (second column) and simulated (third column) results on admission (baseline) with simulated LVAD support at 8900 rpm (fourth column) have been listed in Table 11.

Table 12 Simulation results with Milrinone for Patient #4

Patient #4	LVAD [8900 rpm] + Milrinone (10%) (Simulation)			LVAD [6000 rpm] + Milrinone (10%) (Simulation)		
	Max	Min	Mean	Max	Min	Mean
BP [mmHg]	82	67	71	78	69	71
RA [mmHg]	-	-	3.6	-	-	3.6
RV [mmHg]	60.0	1.0	18.0	59.0	1.0	17.0
PA [mmHg]	-	-	49	-	-	48
PCWP [mmHg]	-	-	30.4	-	-	29
HR [bpm]	78			78		
LVEF	18.3%			18.3%		
BSA [m ²]	1.83			1.83		
CO [L/min]	CO _{VENTR}	1.6		CO _{VENTR}	0.77	
	Q _{VAD}	3.82		Q _{VAD}	4.74	
	Q _{TOT}	5.42		Q _{TOT}	5.51	
CI [L/min/m ²]	0.87			0.42		
TPG [mmHg]	18.6			19.0		
PVR [wood unit]	11.6 (18.6/1.6)			24.68 (19/0.77)		
	4.87 (18.6/3.82)			4.01 (19/4.74)		
RVSWI [g/m ² /beat]	23.44			23.31		
	Simulated			Simulated		
EDV [ml]	225.5			212.4		
ESV [ml]	184.2			178.4		
Ea [mmHg/ml]	2.0			2.3		
Ees[mmHg/ml]	0.515			0.515		
Ea/Ees	3.88			4.47		

The results obtained with simulated LVAD support at 8900 rpm (second column) and 6000 rpm (third column) with Milrinone administration have been listed in Table 12.

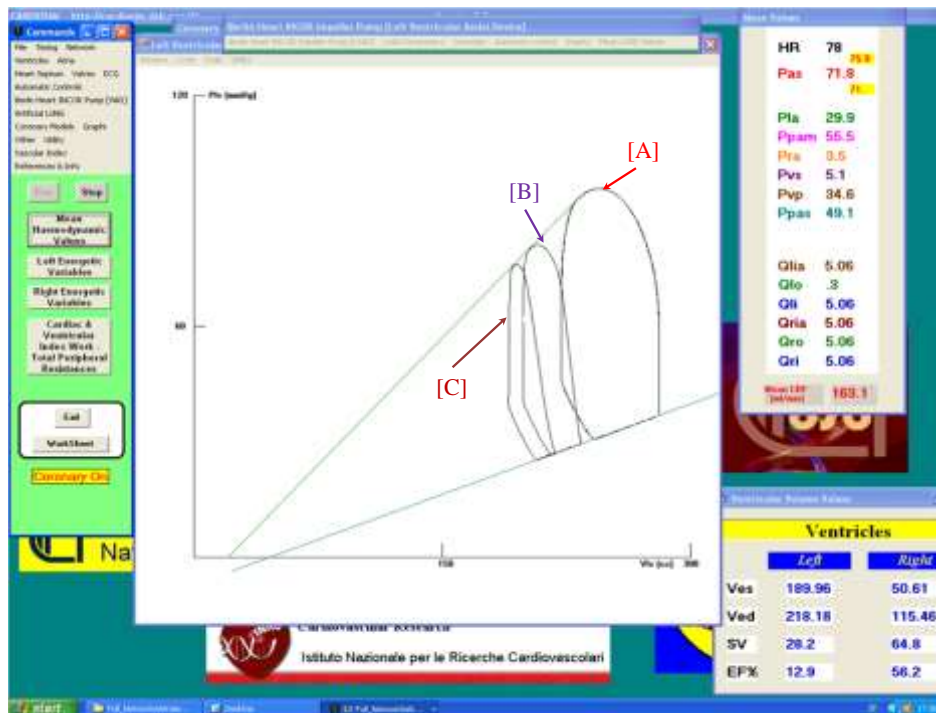


Fig. 10 Screen output obtained from *CARDIOSIM*[®] for Patient #4.

In Fig. 10, the main window compares the cardiac cycle in different situations in terms of PV loops. The [A] loop shows the baseline setting on admission; the [B] loop shows simulated conditions with LVAD at 8900 rpm; the [C] loop shows simulated conditions with LVAD at 6000 rpm. The right upper box shows the simulated mean hemodynamic parameters during LVAD support at 6000 rpm. The right lower box shows EDV, ESV, SV and EF% for both ventricles.

4.5 Patient #5

Tables 13 and 14 show the measured parameters and simulation results obtained for Patient #5. Again, LVAD support at different pump speed (8900 rpm and 6000 rpm) was considered for this patient in view of the patho-physiological background for comparison purposes.

Table 13 Measured parameters and simulation results for Patient #5

Patient #5	Measured [RHC 1]			Simulation [RHC 1]			LVAD [8900 rpm] (Simulation)		
	Max	Min	Mean	Max	Min	Mean	Max	Min	Mean
BP [mmHg]	112	68	82	114	69	82	96.7	76.7	82
RA [mmHg]	-	-	12.0	-	-	6.4	-	-	6.6
RV [mmHg]	71	23	39	59	8.0	21	55	8	20
PA [mmHg]	67	27	43	55	45	50	51	42	47
PCWP [mmHg]	41	20	32	42	14	30	38	10	25.5
HR [bpm]	80			80			80		
LVEF	36%			35.9%			28.8%		
BSA [m ²]	1.88			1.88			1.88		
CO [L/min]	5.4			5.4			CO _{VENTR}	1.86	
							Q _{VAD}	3.78	
							TOT	5.64	
CI [L/min/m ²]	2.87			2.87			0.99		
TPG [mmHg]	11			20			21.5		
PVR [wood unit]	2.04			3.7			11.56 (21.5/1.86)		
							5.68 (21.5/3.78)		
RVSWI [g/m ² /beat]	15.14			21.24			20.6		
	Estimated			Simulated			Simulated		
EDV [ml]	~187.5			188			154.3		
ESV [ml]	~120			120			109.9		
Ea [mmHg/ml]	~1.49			1.6			2.1		
Ees[mmHg/ml]	-			1.0			1.0		
Ea/Ees	-			1.6			2.1		

Table 13 shows measured (second column) and simulated (third column) parameters on admission; simulated parameters obtained with LVAD support at 8900 rpm have been listed in the fourth column.

Table 14 Simulation results with Milrinone for Patient #5

Patient #5	LVAD [8900 rpm] + Milrinone (10%) (Simulation)			LVAD [6000 rpm] + Milrinone (10%) (Simulation)		
	Max	Min	Mean	Max	Min	Mean
BP [mmHg]	90	76.2	79.2	78	69	71
RA [mmHg]	-	-	6.8	-	-	6.8
RV [mmHg]	53.5	2	19.9	52.5	1	19.7
PA [mmHg]	49	39	44	48	38	43.6
PCWP [mmHg]	37.4	10	24	36	9	23
HR [bpm]	80			80		
LVEF	33.2 %			29.5%		
BSA [m ²]	1.88			1.88		
CO [L/min]	CO _{VENTR} 2.19			CO _{VENTR} 1.25		
	Q _{VAD} 3.80			Q _{VAD} 4.78		
	Q _{TOT} 5.99			Q _{TOT} 6.03		
CI [L/min/m ²]	1.16			0.66		
TPG [mmHg]	20.4			20.6		
PVR [wood unit]	5.37 (20.4/3.8)			4.31 (20.6/4.78)		
	9.32 (20.4/2.19)			16.48 (20.6/1.25)		
RVSWI [g/m ² /beat]	20.37			20		
	Simulated			Simulated		
EDV [ml]	146.3			137.7		
ESV [ml]	97.7			96.6		
Ea [mmHg/ml]	1.9			2.2		
Ees[mmHg/ml]	1.1			1.1		
Ea/Ees	1.73			2.0		

Table 14 compares simulated LVAD assistance with Milrinone administration at 8900 rpm (second column) and 6000 rpm (third column).

A graphical representation of PV loops is shown in Fig. 11.

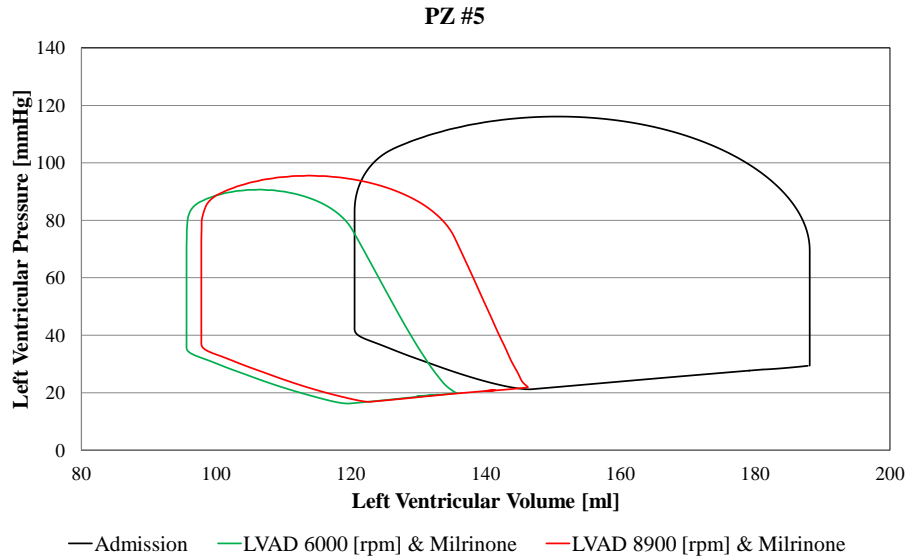


Fig. 11 Graphical representation of the left ventricular PV loop in Patient #5.

The data plotted in Fig. 11 were obtained from the left ventricular instantaneous pressure and volume stored in an Excel file during the simulation. The PV loops represent the cardiac cycle in three specific situations. Conditions on admission are shown in black; simulation conditions with LVAD at 8900 rpm and Milrinone are shown in red; simulation conditions with LVAD at 6000 rpm and Milrinone are shown in green.

4.6 Patient #6

Tables 15 and 16 show measured parameters and simulation results for Patient #6. LVAD support was simulated with higher pump speed values (8900 rpm and 10000 rpm) in view of the background of this patient.

Table 15 Measured parameters and simulation results for Patient #6

Patient #6	Measured [RHC 1]			Simulation [RHC 1]			LVAD [8900 rpm] (Simulation)		
	Max	Min	Mean	Max	Min	Mean	Max	Min	Mean
BP [mmHg]	106	70	82	107	73	82	91.2	89.6	90.6
RA [mmHg]	-	-	14.0	-	-	5	-	-	4.7
RV [mmHg]	57	10	23	64	2	20	54	1	18
PA [mmHg]	68	41	53	55	45	58	49	44	46.7
PCWP [mmHg]	-	-	49	-	-	47	-	-	32.4
HR [bpm]	102			102			102		
LVEF	21%			21%			15.5%		
BSA [m ²]	2.04			2.04			2.04		
CO [L/min]	3.2			3.2			CO _{VENTR}	0	
							Q _{VAD}	3.79	
							Q _{TOT}	3.79	
CI [L/min/m ²]	1.57			1.57			-		
TPG [mmHg]	4			11			14.3		
PVR [wood unit]	1.25			3.44			-		
							3.77 (14.3/3.79)		
RVSWI [g/m ² /beat]	8.16			11.1			10.4		
	Estimated			Simulated			Simulated		
EDV [ml]	~149.4			149.9			103		
ESV [ml]	~118			118			87		
Ea [mmHg/ml]	~3.04			3.3			4.6		
Ees[mmHg/ml]	-			0.961			0.961		
Ea/Ees	-			3.43			4.79		

Table 15 shows measured (second column) and simulated (third column) parameters on admission and parameters obtained with simulated LVAD assistance at 8900 rpm (fourth column).

Table 16 Simulation results with Milrinone for Patient #6

Patient #6	LVAD [8900 rpm] + Milrinone (10%) (Simulation)			LVAD [10000 rpm] + Milrinone (10%) (Simulation)		
	Max	Min	Mean	Max	Min	Mean
BP [mmHg]	88	84	85	93	82	85
RA [mmHg]	-	-	4.7	-	-	4.7
RV [mmHg]	56	1	18	57	2	19
PA [mmHg]	51	46	49	53	48	51
PCWP [mmHg]	-	-	36	-	-	38
HR [bpm]	102			102		
LVEF	16%			18.3%		
BSA [m ²]	2.04			2.04		
CO [L/min]	CO _{VENTR}	0.14		CO _{VENTR}	0.73	
	Q _{VAD}	3.8		Q _{VAD}	3.12	
	Q _{TOT}	3.94		Q _{TOT}	3.85	
CI [L/min/m ²]	0.07			0.36		
TPG [mmHg]	13			13		
PVR [wood unit]	3.42 (13/3.8)			4.17 (13/3.12)		
	92.86 (13/0.14)			17.81 (13/0.73)		
RVSWI [g/m ² /beat]	11.41			11.65		
	Simulated			Simulated		
EDV [ml]	113.4			121		
ESV [ml]	95.3			98.8		
Ea [mmHg/ml]	4.9			4.2		
Ees[mmHg/ml]	1.057			1.057		
Ea/Ees	4.64			3.97		

Table 16 compares parameters obtained with LVAD support at 8900 rpm (second column) and 10000 rpm (third column) following Milrinone administration.

A graphical representation of these data is shown in Fig. 12.

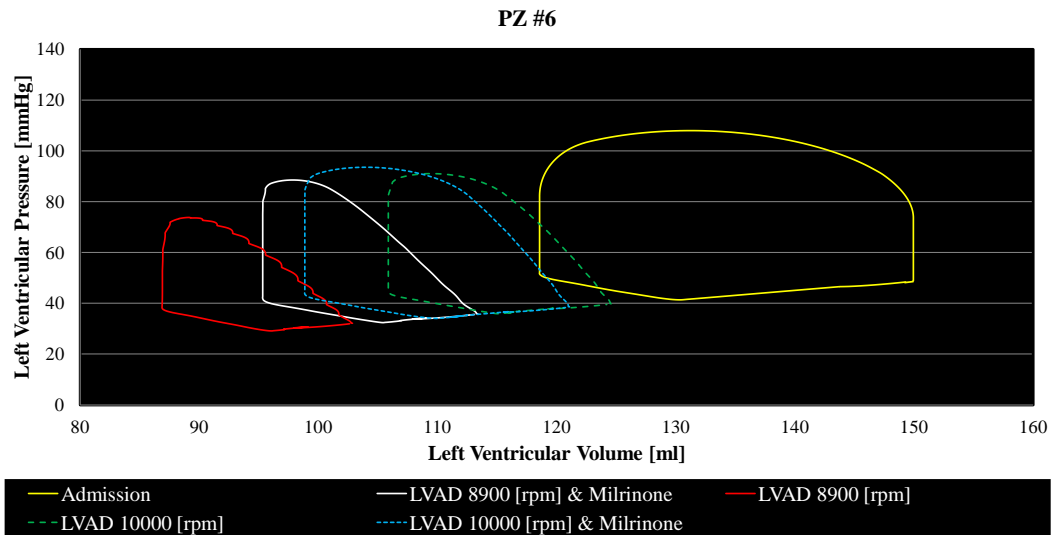


Fig. 12 Graphical representation of the PV loop in Patient #6.

Data were obtained from the left ventricular instantaneous pressure and volume stored in an Excel file during the simulation. The PV loops in Fig.12 represent the cardiac cycle in five specific situations. The yellow line shows the admission conditions; the green dashed line shows simulated conditions with LVAD support at 10000 rpm; the blue dashed line shows simulated conditions with LVAD support at 10000 rpm and Milrinone; the white line shows simulated conditions with LVAD support at 8900 rpm and Milrinone; the red line shows simulated conditions with LVAD support at 8900 rpm.

We also compared the changes in Coronary Blood Flow (CBF) in the last three patients. The outcome is shown in Fig. 13.

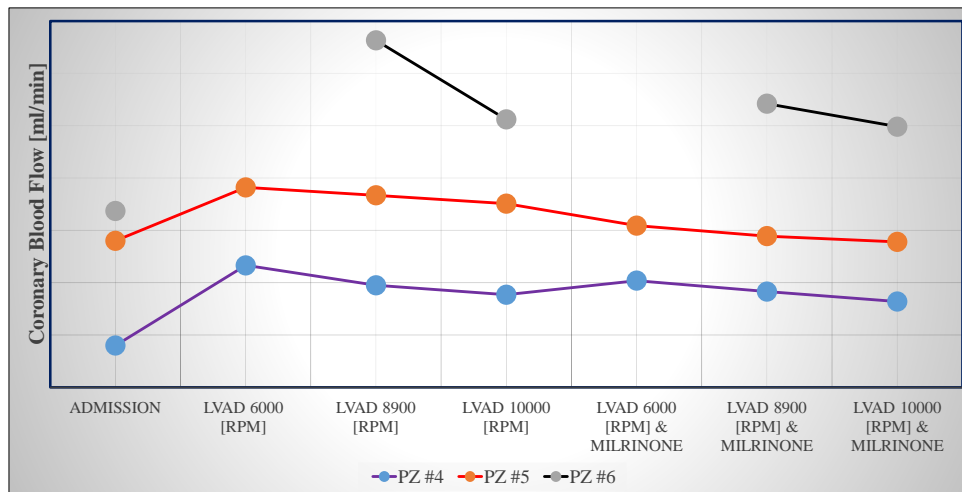


Fig. 13 Graphical representation of CBF in Patients #4, #5 and #6.

Data were obtained from the left ventricular instantaneous pressure and volume stored in an Excel file during the simulation and subsequently manipulated to show the trend in Fig. 13. The blue line represents Patient #4, the orange line represents Patient #5 and the black line represents Patient #6. The values of CBF were calculated (from left to right) on admission; LVAD assistance at 6000 rpm; LVAD assistance at 8900 rpm; LVAD assistance at 10000 rpm; LVAD assistance at 6000 and Milrinone; LVAD assistance at 8900 rpm and Milrinone; LVAD assistance at 10000 rpm and Milrinone. CBF results at 6000 rpm for Patient #6 are not included because the patho-physiological background did not allow appropriate calculations at this specific setting.

4.7 Discussion

Cardiovascular modelling has been very successful in increasing our knowledge of physiological mechanisms where simplified representations of complex biological systems can be used to study their behaviour at different levels [57][98][99]. Although still far from clinical application on a daily basis [7][78], patient-specific modelling has consistently shown significant potential [27][29][71]. Barriers to further clinical implementation include validation against in vivo data with uncertainty quantification, the need for large-scale clinical trials to show reliability with improved outcome and the need for more efficient modelling and simulation methods [61]. To overcome scepticism and gain wide acceptance, a model should be robust, realistic enough and easy to understand with the ability to deliver within the time and constraints of clinical practice. Our aim is to use modelling and simulation as an additional tool to guide therapeutic intervention or predict clinical outcome: the clinician will remain the ultimate decision-maker.

A simulation-based approach in the context of advanced heart failure with patient-specific modelling as a preoperative strategy may be an additional tool to obtain accurate predictions of device performance in a clinical setting and treatment optimization of these patients. Management of advanced heart failure is demanding in view of the complex and challenging nature of this group of patients with often critical clinical presentation.

My experience at the Cardiovascular Hybrid/Modelling Lab has been highly educational. Although at first it was quite intimidating to understand the principles behind a simulation approach and its clinical application based on a software like CARDIOSIM[®], which is not familiar to someone who has been exposed to medical training, my enthusiasm and willingness to learn made me soon enjoy the novelty of the subject. Nevertheless, the patience and the guidance of Dr. De Lazzari allowed me to acquire the basic skills which have made me quite conversant with the use of the software. During the past few months, I have had the opportunity to work on an interesting topic with an active and stimulating research group who has contributed to increase my knowledge and develop a different attitude with a more complete approach towards complex clinical problems which I believe will be useful in my future career as a clinician.

We have concentrated our efforts on a retrospective analysis of hemodynamic data obtained from six heart failure patients with different background. Data availability for the right heart was limited; therefore, our simulations were more accurate for the left heart in terms of hemodynamic parameters.

Although some of the baseline parameters on admission for Patient #1 (such as RA, RV and PVR) could not be correctly estimated by the simulator, the outcome after LVAD support showed a reduction in EDV (10%) and in ESV (16%) leading to a leftward shift of the left PV loop. This unloading of the left ventricle was also reflected on the PA pressure, which showed a 2.5% reduction from its baseline simulated value. The arterial elastance (E_a) decreased to 2.6 mmHg/ml and the E_a/E_{es} ratio decreased to 2.95. These effects were induced by the presence of the pump with changes in total peripheral resistance. The total CO improved slightly reaching a value of 2.82 L/min with only 0.67 L/min provided by the native ventricle and the remaining 2.15 L/min provided by the LVAD. Further increase Q_{TOT} was not observed despite changes in the LVAD rotational speed. The LVEF showed a slight increase to 31.4% although further improvement would be usually observed over a period of time [10]. Due to the complex background of this particular patient and the potential development of comorbidities-related complications, the clinical decision to continue with medical management would be appropriate although recent evidence supporting the “obesity paradox” in cardiac surgery may lead to further argument in favour of LVAD insertion.

Simulation of the hemodynamic status on admission showed comparable mean values with those measured during right heart catheterization in Patient #2. LVAD assistance showed significantly improved left ventricular EF, particularly after Milrinone administration (49.8% vs. 55.9%) with a reduction in EDV (9%) and in ESV (8%) and a subsequent leftward shift of the PV loop. Global cardiac performance also improved as demonstrated by the slight decrease in the E_a/E_{es} ratio to 1.32 (1.2 with Milrinone) and in E_a (0.9 mmHg/ml). Q_{TOT} was

5.39 (5.96 with Milrinone) L/min, with 1.72 (2.04 with Milrinone) L/min provided by the native ventricle and 3.67 (3.92) L/min provided by LVAD simulation.

Despite some variability between measured and simulated parameters on admission, the outcome after the simulations was mostly favourable in Patient #3. The left ventricular EF increased after LVAD assistance (and Milrinone administration) to 19% (22%) with 14% reduction in EDV (16%), 18% reduction in ESV (22.5%) and a leftward shift of the PV loop. The lower E_a , which decreased to 1.3 (1.2 with Milrinone) mmHg/ml, led to a better ventricular-arterial coupling where the E_a/E_{es} ratio decreased to 3.25 (2.73) from its simulated starting value of 4.75. Q_{TOT} was 4.54 (5.15 with Milrinone) L/min, with 3.8 (4.22) L/min provided by the LVAD and 0.74 (0.93) L/min provided by the native ventricle.

Simulated admission parameters showed comparable mean values with those measured during right heart catheterization in Patient #4. The LVEF decreased to 15% after LVAD assistance at 8900 rpm (18.3% with Milrinone administration; 18.3% at 6000 rpm with Milrinone administration), with 18% reduction in EDV (19.5%; 24%), 10% reduction in ESV (17%; 19.5%) and a leftward shift of the PV loop. E_a increased to 2.3 mmHg/ml at 8900 rpm (2.0 with Milrinone; 2.3 at 6000 rpm with Milrinone) with an increase in E_a/E_{es} ratio to 4.91 (3.88; 4.47). Q_{TOT} was 4.95 L/min at 8900 rpm (5.42 with Milrinone; 5.42 at 6000 rpm with Milrinone) with 1.13 (1.6; 0.77) L/min provided by the native left ventricle and 3.82 (3.82; 4.74) L/min provided by the LVAD.

Some variability between measured and simulated admission parameters was observed in Patient #5 with particular reference to the right heart hemodynamic parameters. The LVEF dropped to 28.8% during LVAD support at 8900 rpm (33.2% with Milrinone; 29.5% at 6000 rpm with Milrinone) with 18% reduction in EDV (22%; 28%), 8.5% reduction in ESV (18.5%, 20.5%) and a leftward shift of the PV loop. E_a increased to 2.1 mmHg/ml at 8900 rpm (1.9 with Milrinone; 2.2 at 6000 rpm with Milrinone) with concomitant increase in the E_a/E_{es} ratio to 2.1 (1.73; 2.0). Q_{TOT} was 5.64 L/min at 8900 rpm (5.42 with Milrinone; 6.03 at 6000 with Milrinone) with 1.86 (1.6; 1.25) L/min provided by the left ventricle and 3.78 (3.82; 4.78) L/min provided by LVAD support.

A difference was observed between some simulated and admission parameters (such as RA, PA, PVR) in Patient #6. The left ventricular EF decreased to 15.5% during simulated LVAD support at 8900 rpm (16% with Milrinone; 18.3 at 10000 rpm with Milrinone) with 31% reduction in EDV (24.5%; 19%), 26% reduction in ESV (19%; 16%) and subsequent leftward shift of the PV loop. PCWP dropped to 32.4 (36; 38) mmHg; PA pressure also dropped to 32.4 mmHg during LVAD assistance at 8900 rpm. E_a increased to 4.6 mmHg/ml at 8900 rpm (4.9 with Milrinone; 4.2 at 10000 rpm with Milrinone) leading to an increase in E_a/E_{es} ratio to 4.79 (4.64; 3.97). Q_{TOT} increased to 3.79 L/min during LVAD assistance at 8900 rpm (3.93 with Milrinone; 3.85 at 10000 rpm with Milrinone), but with no flow (0.07; 0.36 L/min) provided by the native ventricle and 3.79 (3.8; 3.12) L/min provided entirely by simulated LVAD assistance.

Overall, the outcome of the simulations showed results that are consistent with the decisions made by Multidisciplinary Team Meetings: the first three patients were confirmed to be unsuitable for LVAD implantation, while the remaining three patients all underwent LVAD implantation.

CHAPTER 5: STATISTICAL ANALYSIS

The accuracy of CARDIOSIM[®] was evaluated through the program Stata[®] using a Student's t-test and a Mann-Whitney test as a check. We selected some of the measured and simulated baseline parameters and a p-value < 0.05 was considered statistically significant.

If there was concordance between the two tests, we selected the p-value from the t-test; if not, we selected the p-value from the Mann-Whitney test, which is the most accurate for our study since it is a non-parametric test. Results for:

- ✚ BP max (systolic blood pressure) show that the p-value from the t-test is 0.32. The results of the two tests are concordant in confirming the accuracy of CARDIOSIM[®] in reproducing this parameter.
- ✚ BP min (diastolic blood pressure) show that the p-value from the Mann-Whitney test is 0.42, confirming again the accuracy of CARDIOSIM[®] in reproducing this parameter. However, the results of the t-test are discordant, showing a statistical significance that is consistent with the tendency of the diastolic blood pressure to show a “normal distribution” among the population. This means that, increasing the sample size indefinitely, we would obtain a very slight overestimation of the parameter.
- ✚ RA (right atrial pressure) show that the p-value from the Mann-Whitney test is 0.01 and, comparing the measured and simulated “median values”, it confirms that there is a slight underestimation of the parameter made by CARDIOSIM[®].
- ✚ RV (right ventricular pressure) show that the p-value from the Mann-Whitney test is 0.07, showing again the accuracy of CARDIOSIM[®] in reproducing the parameter.
- ✚ PA (pulmonary arterial pressure) show that the p-value from the t-test is 0.73. The results of the two tests are again concordant in confirming the accuracy of CARDIOSIM[®] in reproducing this parameter.
- ✚ PCWP (pulmonary capillary wedge pressure) show that the p-value from the Mann-Whitney test is 0.29, demonstrating again the accuracy of CARDIOSIM[®] in reproducing this parameter.
- ✚ LVEF (left ventricular ejection fraction) are shown in Fig. 14 and 15.

```

. sum lvefmeasured, det

-----+-----
LVEF% measured
-----+-----
Percentiles      Smallest
1%               15           15
5%               15           21
10%              15           21
25%              21           27
50%              24           Largest
75%              36           21
90%              45           27
95%              45           36
99%              45           45

Obs               6
Sum of Wgt.       6
Mean              27.5
Std. Dev.         11.13104
Variance          123.9
Skewness          .5514019
Kurtosis          1.985408

. sum lvefsimulated, det

-----+-----
LVEF% simulated
-----+-----
Percentiles      Smallest
1%               15           15
5%               15           21
10%              15           21
25%              21           26.9
50%              27.94          Largest
75%              35.9           21
90%              45.1           26.9
95%              45.1           35.9
99%              45.1           45.1

Obs               6
Sum of Wgt.       6
Mean              27.48333
Std. Dev.         11.14835
Variance          124.2857
Skewness          .5649593
Kurtosis          2.006635

. ttest lvefmeasured== lvefsimulated

Paired t test
-----+-----
Variable |      Obs      Mean  Std. Err.  Std. Dev.  [95% Conf. Interval]
-----+-----
lvefme-d |         6      27.5   4.544227   11.13104   15.81869   39.18131
lvefai-d |         6    27.48333   4.551294   11.14835   15.78386   39.18281
-----+-----
diff |         6   -0.16667   .0307315   .0752765   -0.623312   .0956646

      mean(diff) = mean(lvefmeasured - lvefsimulated)      t = 0.5423
      Ho: mean(diff) = 0                                degrees of freedom = 5

      Ha: mean(diff) < 0                                Ha: mean(diff) != 0                                Ha: mean(diff) > 0
      Pr(T < t) = 0.6946                                Pr(|T| > |t|) = .                                Pr(T > t) = 0.3054

ranksum lvefmeasured_01, by(var5)

Two-sample Wilcoxon rank-sum (Mann-Whitney) test
-----+-----
var5 |      obs  rank sum  expected
-----+-----
  0 |         6      39.5      39
  1 |         6      38.5      39
-----+-----
combined |      12      78      78

unadjusted variance      39.00
adjustment for ties      -1.50
-----+-----
adjusted variance      37.50

Ho: lvefm-01(var5==0) = lvefm-01(var5==1)
      z = 0.082
      Prob > |z| = 0.9349

```

Fig. 14 Screen output obtained from the software Stata[®] for LVEF%. In green are shown the median values, in blue the mean values, in red the p-value from the t-test, in yellow the p-value from the Mann-Whitney test

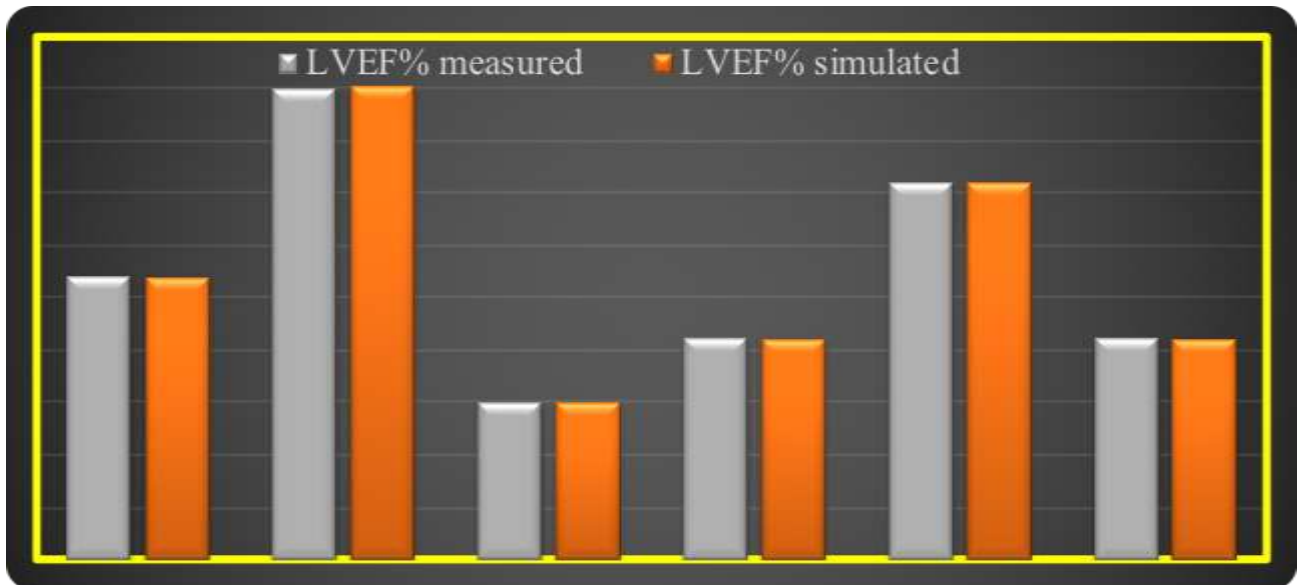


Fig. 15 Comparison between measured and simulated LVEF% values

The p-value from the t-test is 0.61, with both tests concordant in confirming the accuracy of CARDIOSIM[®] in reproducing this parameter. Moreover, as shown in Fig. 14, the measured and simulated “mean” and “median” values are almost identical.

- + EDV (end-diastolic volume) show that the p-value from the t-test is 0,66. Also in this case, the results of the two tests are concordant in confirming the accuracy of CARDIOSIM[®] in reproducing this parameter.
- + ESV (end-systolic volume) show that the p-value from the t-test is 0.48, with both tests confirming the accuracy of CARDIOSIM[®] in reproducing this parameter. The measured “mean” and “median” values are again very similar.
- + Ea (arterial elastance) show that the p-value from the Mann-Whitney test is 0.37, confirming of the accuracy of CARDIOSIM[®] in reproducing also this parameter.

CHAPTER 6: CONCLUSIONS

Although previous experience, co-morbidities and the risk of potentially fatal complications are all crucial factors to be considered in clinical decision-making, the use of patient-specific modelling may become a daily approach to aid the clinician towards the most suitable treatment. Moreover, the role of simulation might be particularly useful in fragile patients, such as children and the elderly, who may benefit from a non-invasive approach for multiple reproductions of their baseline hemodynamic parameters.

Despite the preliminary nature of this study and the limited number of patients considered, CARDIOSIM[®] has the potential to deliver reliable simulations for a more quantitative and critical evaluation of device treatment and optimization in advanced heart failure.

The clinician remains the ultimate decision-maker but relies on an additional tool that may reduce unnecessary guess work and perhaps give reassurance and possibly reduce uncertainty.

REFERENCES

1. Aaronson KD, Schwartz JS, Chen T-M et al. Development and Prospective Validation of a Clinical Index to Predict Survival in Ambulatory Patients Referred for Cardiac Transplant Evaluation. *Circulation* 1997; 95: 2660-2667.
2. AbouEzzeddine OF, French B, Mirzoyev SA et al. From statistical significance to clinical relevance: A simple algorithm to integrate brain natriuretic peptide and the Seattle Heart Failure Model for risk stratification in heart failure. *J Heart Lung Transplant* 2016; 35: 714-721.
3. Antaki JF, Poirier V, Pagani FD. Engineering Concepts in the Design of Mechanical Circulatory Support. In: *Mechanical Circulatory Support*. Frazier OH, Kirklin JK ed.; ISHLT Monograph Series, New York, Elsevier; 2006, pp. 33-52.
4. Arnold WS, Bourque K. The engineer and the clinician: Understanding the work output and troubleshooting of the HeartMate II rotary flow pump. *J Thorac Cardiovasc Surg* 2013; 145: 32-36.
5. Birks EJ, Tansley PD, Yacoub MH et al. Incidence and Clinical Management of Life-Threatening Left Ventricular Assist Device Failure. *J Heart Lung Transplant* 2004; 23: 964-969.
6. Blanc JJ, Bertault-Valls V, Fatemi M et al. Midterm benefits of left univentricular pacing in patients with congestive heart failure. *Circulation*. 2004; 109(14): 1741-4.
7. Bluestein D. Utilizing Computational Fluid Dynamics in Cardiovascular Engineering and Medicine – What You Need to Know. Its Translation to the Clinic/Bedside. *Artificial Organs* 2017; 41(2): 117-121.
8. Bolno PB, Kresh JY. Physiologic and haemodynamic basis of ventricular assist devices. *Cardiol Clin* 2003; 21: 15-27.
9. Boyle AJ, Ascheim DD, Russo MJ et al. Clinical outcomes for continuous flow left ventricular assist device patients stratified by pre-operative INTERMACS classification. *J Heart Lung Transplant* 2011; 30(4): 402-407.
10. Capoccia M, Bowles CT, Sabashnikov A et al. A UK single centre retrospective analysis of the relationship between haemodynamic changes and outcome in patients undergoing prolonged left ventricular assist device support. *Ann Thorac Cardiovasc Surg*. 2015; 21: 151–6.
11. Capoccia M, Marconi S, Singh SA et al. Simulation as a preoperative planning approach in advanced heart failure patients. A retrospective clinical analysis. *BioMed Eng OnLine* 2018; 17: 52.
12. Capoccia M, Marconi S, De Lazzari C. Decision-making in advanced heart failure patients requiring LVAD insertion: can preoperative simulation become the way forward? A case study. *Journal of Biomedical Engineering and Informatics*, 4 (2), <https://doi.org/10.5430/jbei.v4n2p8>.
13. Cikes M, Solomon SD. Beyond ejection fraction: an integrative approach for assessment of cardiac structure and function in heart failure. *Eur Heart J* 2016; 37: 1642-1650.

14. Cook JL, Colvin M, Francis GS et al. Recommendations for the Use of Mechanical Circulatory Support: Ambulatory and Community Patient Care: A Scientific Statement From the American Heart Association. *Circulation*. 2017; 135(25): e1145-e1158.
15. Cowger J, Sundareshwaran K, Rogers JG et al. Predicting survival in patients receiving continuous flow left ventricular assist devices: the HeartMate II risk score. *J Am Coll Cardiol* 2013; 61: 313–321.
16. Darowski M, De Lazzari C, Ferrari G et al. The influence of simultaneous intra-aortic balloon pumping and mechanical ventilation on hemodynamic parameters – numerical simulation. *Front Med Biol Eng* 1999; 9(2): 155-74.
17. De Lazzari C, D'Ambrosi A, Tufano F et al. Cardiac Resynchronization Therapy: could a numerical simulator be a useful tool in order to predict the response of the biventricular pacemaker synchronization? *Eur Rev Med Pharmacol Sci* 2010; 14(11): 969-978.
18. De Lazzari C, Darowski M, Ferrari G et al. Ventricular energetics during mechanical ventilation and intra-aortic balloon pumping-computer simulation. *J Med Eng Technol* 2001; 25(3): 103-111.
19. De Lazzari C, Darowski M, Ferrari G, Clemente F. The influence of left ventricle assist device and ventilatory support on energy-related cardiovascular variables. *Med Eng Phys* 1998; 20(2): 83-91.
20. De Lazzari C, Darowski M, Ferrari G et al. Modelling in the study of interaction of Hemopump device and artificial ventilation. *Comput. in Biol. and Med.* 2006; 45(5): 1235-1251.
21. De Lazzari C, Darowski M, Ferrari G et al. The impact of rotary blood pump in conjunction with mechanical ventilation on ventricular energetic parameters: Numerical Simulation. *Methods Inf. Med.* 2006; 45: 574-583.
22. De Lazzari C, Ferrari G, Mimmo R et al. A desk-top computer model of the circulatory system for heart assistance simulation: effect of a LVAD on energetic relationships inside the ventricle. *Med Eng Phys* 1994; 16(2): 97-103.
23. De Lazzari C, Genuini I, Pisanelli DM et al. Interactive simulator for e-Learning environments: a teaching software for health care professionals. *BioMedical Engineering OnLine* 2014; 13: 172.
24. De Lazzari C, Pirckhalava M (Eds). *Cardiovascular and Pulmonary Artificial Organs: Educational Training Simulators*. Rome, Consiglio Nazionale delle Ricerche (CNR) Press, 2017.
25. De Lazzari C, Quatember B. Cardiac Energetics in Presence of Lung Assist Devices: In Silico Study. *Model Num Sim Mater Sci* 2016; 6: 41-57.
26. Doost SN, Zhong L, Morsi YS. Ventricular Assist Devices: Current State and Challenges. *J Med Devices* 2017; 11: 040801-1-040801-11.
27. Doshi D, Burkhoff D. Cardiovascular Simulation of Heart Failure. *Pathophysiology and Therapeutics*. *J Card Fail* 2016; 22(4): 303-311.
28. Drakos SG, Terrovitis JV, Anastasiou-Nana MI et al. Reverse remodeling during long-term mechanical unloading of the left ventricle. *J Mol Cell Cardiol*. 2007; 43: 231–242.
29. Duanmu Z, Yin M, Fan X et al. A patient-specific lumped-parameter model of coronary circulation. *SCIENTIFIC REPORTS* 2018; 8: 874.

30. Emergy RW, Joyce LD. Directions in cardiac assistance. *J Card Surg* 1991; 6: 400-414.
31. Estep JD, Starling RC, Horstmanshof DA et al. Risk assessment and comparative effectiveness of left ventricular assist device and medical management in ambulatory heart failure patients: results from the ROADMAP study. *J Am Coll Cardiol* 2015; 66: 1747–1761.
32. Feldman D, Pamboukian SV, Teuteberg JJ et al. The 2013 International Society for Heart and Lung Transplantation Guidelines for mechanical circulatory support: executive summary. *J Heart Lung Transplant* 2013; 32: 157–187.
33. Ferrari G, De Lazzari C, Mimmo R et al. A modular numerical model of the cardiovascular system for studying and training in the field of cardiovascular physiopathology. *J Biomed Eng* 1992; 14: 91-107.
34. Fitzpatrick JR 3rd, Frederick JR, Hsu VM et al. Risk score derived from pre-operative data analysis predicts the need for biventricular mechanical circulatory support. *J Heart Lung Transplant* 2008; 27: 1286-92.
35. Frolov SV, Sindeev SV, Lischouk VA et al. A lumped parameter model of cardiovascular system with pulsating heart for diagnostic studies. *J Mech Med Biol* 2016 17(3), <https://doi.org/10.1142/S0219519417500567>.
36. Fonarow GC, Hsu JJ. Left Ventricular Ejection Fraction. What is “Normal”? *JACC: Heart Failure* 2016; 4(6): 511-513.
37. Gerber Y, Weston SA, Redfield MM, et al. A contemporary appraisal of the heart failure epidemic in Olmsted County, Minnesota, 2000 to 2010. *JAMA Intern Med* 2015; 175: 996–1004.
38. Gustafsson F, Rogers JG. Left ventricular assist device therapy in advanced heart failure: patient selection and outcomes. *Eur J Heart Fail* 2017; 19(5): 595-602.
39. Heatley G, Sood P, Goldstein D et al. and on behalf of the MOMENTUM 3 Investigators. Clinical trial design and rationale of the Multicenter Study of MagLev Technology in Patients Undergoing Mechanical Circulatory Support Therapy with HeartMate 3 (MOMENTUM 3) investigational device exemption clinical study protocol. *J Heart Lung Transplant* 2016; 35: 528-536.
40. Holman WL, Naftel DC, Eckert CE et al. Durability of left ventricular assist devices: Interagency Registry for Mechanically Assisted Circulatory Support (INTERMACS) 2006 to 2011. *J Thorac Cardiovasc Surg* 2013; 146: 437-441.
41. Jaski BE, Fifer MA, Wright RF et al. Positive inotropic and vasodilator actions of milrinone in patients with severe congestive heart failure. Dose-response relationships and comparison to nitroprusside. *J Clin Invest*, 1985; 75(2): 643-649.
42. Jorde UP, Kushwaha SS, Tatoes AJ et al. Results of the destination therapy post-Food and Drug Administration approval study with a continuous flow left ventricular assist device: a prospective study using the INTERMACS registry (Interagency Registry for Mechanically Assisted Circulatory Support). *J Am Coll Cardiol* 2014; 63: 1751–1757.
43. Katz AM, Rolett EL. Heart failure: when form fails to follow function. *Eur Heart J* 2016; 37: 449-454.
44. Katz AM. Heart Failure. Pathophysiology, Molecular Biology and Clinical Management. Lippincott William & Wilkins, Philadelphia, 2000.

45. Ketchum ES, Jacobson AF, Caldwell JH et al. Selective improvement in Seattle Heart Failure Model risk stratification using iodine-123 meta-iodobenzylguanidine imaging. *J Nuclear Cardiol* 2012; 19(5): 1007-1016.
46. Kirk JA, Kass DA. Electromechanical dyssynchrony and resynchronization of the failing heart. *Circ Res.* 2013; 113: 765-776.
47. Kirklin JK, Naftel DC, Kormos RL et al. Fifth INTERMACS annual report: Risk factor analysis from more than 6,000 mechanical circulatory support patients. *J Heart Lung Transplant* 2013; 32: 141-156.
48. Kirklin JK, Naftel DC, Pagani FD et al. Long-term mechanical circulatory support (destination therapy): On track to compete with heart transplantation? *J Thorac Cardiovasc Surg* 2012; 144: 584-603.
49. Kirklin JK, Naftel DC, Pagani FD et al. Sixth INTERMACS annual report: a 10,000-patient database. *J Heart Lung Transplant* 2014; 33: 555-564.
50. Kohn LT, Corrigan JM, Donaldson MS. *To err is human: Building a safer health system.* Washington DC: National Academy Press; 1999.
51. Kokalari I, Kara T, Guerrisi M. Review on lumped parameter method for modeling the blood flow in systemic arteries. *Journal of Biomedical Science and Engineering* 2013; 6: 92-99.
52. Kormos RL, Teuteberg JJ, Pagani FD et al. for the HeartMate II Clinical Investigators. Right ventricular failure in patients with the HeartMate II continuous flow left ventricular assist device: Incidence, risk factors, and effect on outcomes. *J Thorac Cardiovasc Surg* 2010; 139: 1316-1324.
53. Langdale LA, Schaad D, Wipf J et al. Preparing Graduates for the First Year of Residency: Are Medical Schools Meeting the Need? *Acad Med.* 2003; 78:39-44.
54. Levy WC, Mozaffarian D, Linker DT et al. on behalf of the REMATCH Investigators. Can the Seattle Heart Failure Model Be Used to Risk-stratify Heart Failure Patients for Potential Left Ventricular Assist Device Therapy? *J Heart Lung Transplant* 2009; 28: 231-236.
55. Levy WC, Mozaffarian D, Linker DT et al. The Seattle Heart Failure Model. Prediction of Survival in Heart Failure. *Circulation* 2006; 113: 1424-1433.
56. Levy WC. Seattle Heart Failure Model. *Am J Cardiol* 2013; 111(8): 1235.
57. Lumens J, Leenders GE, Cramer MJ et al. Mechanistic evaluation of echocardiographic dyssynchrony indices: patient data combined with multiscale computer simulations. *Circ Cardiovasc Imaging.* 2012; 5: 491-9.
58. Lüscher TF, Enseleit F, Pacher R et al. Haemodynamic and neurohumoral effects of selective endothelin A (ET(A)) receptor blockade in chronic heart failure: the Heart Failure ET(A) Receptor Blockade Trial (HEAT). *Circulation.* 2002; 106(21); 2666-72.
59. Mancini D, Colombo PC. Left ventricular assist devices: a rapidly evolving alternative to transplant. *J Am Coll Cardiol.* 2015; 65: 2542-55.
60. Mariscalco G, Wozniak MJ, Dawson AG et al. Body mass index and mortality among adults undergoing cardiac surgery. a nationwide study with a systematic review and meta-analysis. *Circulation.* 2017; 135: 850-63.

61. Marsden AL, Esmaily-Moghadam M. Multiscale Modelling of Cardiovascular Flows for Clinical Decision Support. *Appl Mech Rev* 2015; 67: 030804-1-030804-11.
62. Martens P, Vercammen J, Ceysens W et al. Effects of intravenous home dobutamine in palliative end-stage heart failure on quality of life, heart failure hospitalization, and cost expenditure. *ESC Heart Fail.* 2018; doi: 10.1002/ehf2.12248.
63. Matthews JC, Koelling TM, Pagani FD, Aaronson KD. The right ventricular failure risk score a pre-operative tool for assessing the risk of right ventricular failure in left ventricular assist device candidates. *J Am Coll Cardiol* 2008; 51: 2163-72.
64. Maybaum S, Williams M, Barbone A et al. Assessment of synchrony relationships between the native left ventricle and the HeartMate left ventricular assist device. *J Heart Lung Transplant* 2002; 21(5): 509-515.
65. McMurray JJV, Packer M, Desai AS. Angiotensin-neprilysin inhibition versus enalapril in heart failure. *N Engl. J. Med.* 2014; 371: 993–1004.
66. Mehra MR, Canter CE, Hannan MM et al. The 2016 International Society for Heart Lung Transplantation listing criteria for heart transplantation: a 10-year update. *J Heart Lung Transplant* 2016; 35:1–23.
67. Mehra MR, Kobashigawa J, Starling R, et al. Listing criteria for heart transplantation: International Society for Heart and Lung Transplantation guidelines for the care of cardiac transplant candidates—2006. *J Heart Lung Transplant.* 2006; 25: 1024-42.
68. Mette S. Olufsen and Ali Nadim. On deriving lumped models for blood flow and pressure in the systemic arteries. *J. Math. Biosci. Eng.* 2004; 1: 61-68.
69. Milisic V and Quarteroni A. Analysis of lumped parameter models for blood flow simulations and their relation with 1D models. *Mathem Mod. And Num. Analysis* 2004; 38: 613-632.
70. Miller LW, Pagani FD, Russell SD, et al. for the HeartMate II Clinical Investigators. Use of a Continuous-Flow Device in Patients Awaiting Heart Transplantation. *N Engl J Med* 2007; 357: 885-896.
71. Morris PD, Narracott A, von Tengg-Kobligk H, et al. Computational fluid dynamics modelling in cardiovascular medicine. *Heart* 2016; 102: 18-28.
72. Morshuis M, El-Banayosy A, Arusoglu L, et al. European experience of Duraheart™ magnetically levitated centrifugal left ventricular assist system. *Eur J Cardiothorac Surg* 2009; 35: 1020-1028.
73. Mozaffarian D, Benjamin EJ, Go AS, et al. and on behalf of the American Heart Association Statistics Committee and Stroke Statistics Subcommittee. Executive summary: heart disease and stroke statistics – 2016 update: a report from the American Heart Association. *Circulation* 2016; 133: 447-454.
74. Netuka I, Sood P, Pya Y, et al. Fully Magnetically Levitated Left Ventricular Assist System for Treating Advanced HF. A Multicenter Study. *J Am Coll Cardiol* 2015; 66: 2579-2589.
75. Pagani FD, Long JW, Dembitsky WP, et al. Improved Mechanical Reliability of the HeartMate XVE Left Ventricular Assist System. *Ann Thorac Surg* 2006; 82: 1413-1418.

76. Pagani FD, Miller LW, Russell SD, et al. HeartMate II Investigators. Extended Mechanical Circulatory Support With a Continuous-Flow Rotary Left Ventricular Assist Device. *J Am Coll Cardiol* 2009; 54: 312-321.
77. Park SJ, Tector A, Piccioni W, et al. Left ventricular assist devices as destination therapy: A new look at survival. *J Thorac Cardiovasc Surg* 2005; 129: 9-17.
78. Pedrizzetti G, Domenichini F. Left Ventricular Fluid Mechanics: The Long Way from Theoretical Models to Clinical Applications. *Ann Biomed Eng* 2015; 43(1): 26-40.
79. Ponikowski P, Voors AA, Anker SD, et al. 2016 ESC Guidelines for the diagnosis and treatment of acute and chronic heart failure: the Task Force for the diagnosis and treatment of acute and chronic heart failure of the European Society of Cardiology (ESC). Developed with the special contribution of the Heart Failure Association (HFA) of the ESC. *Eur J Heart Fail* 2016; 18: 891–975.
80. Rose EA, Gelijns AC, Moskowitz AJ, et al. for the Randomized Evaluation of Mechanical Assistance for the Treatment of Congestive Heart Failure (REMATCH) Study Group. Long-Term Use Of A Left Ventricular Assist Device For End-Stage Heart Failure. *N Engl J Med* 2001; 345(20): 1435-1443.
81. Rose EA, Moskowitz AJ, Packer M, et al. for the REMATCH Investigators. The REMATCH Trial: Rationale, Design, and End Points. *Ann Thorac Surg* 1999; 67: 723-730.
82. Sagawa K, Maughan L, Suga H, Sunagawa K. Cardiac contraction and the Pressure-Volume relationships. 1988 Oxford University Press, New York.
83. Schmid Daners M, Kaufmann F, Amacher R, et al. Left Ventricular Assist Devices: Challenges Toward Sustaining Long-Term Patient Care. *Ann Biomed Eng* 2017; 45(8): 1836-1851.
84. Sheikh FH, Russell SD. HeartMate® II continuous-flow left ventricular assist system. *Expert Rev Med Devices* 2011; 8: 11-21.
85. Siess T, Reul H. Basic Design Criteria for Rotary Blood Pumps. In: *Rotary Blood Pumps. New Developments and Current Applications*. Matsuda H ed.; Tokyo, Springer-Verlag, 2000, pp 69-83.
86. Slaughter MS, Pagani FD, Rogers JG, et al. for the HeartMate II Clinical Investigators. Clinical management of continuous-flow left ventricular assist devices in advanced heart failure. *J Heart Lung Transplant* 2010; 29: S1-S39.
87. Slaughter MS, Rogers JG, Milano CA, et al. for the HeartMate II Investigators. Advanced Heart Failure Treated with Continuous-Flow Left Ventricular Assist Device. *N Engl J Med* 2009; 361: 2241-2251.
88. Stevenson LW, Pagani FD, Young JB, et al. INTERMACS Profiles of Advanced Heart Failure: The Current Picture. *J Heart Lung Transplant* 2009; 28: 535-541.
89. Strueber M, O'Driscoll G, Jansz P, et al. for the HeartWare Investigators. Multicenter Evaluation of an Intrapericardial Left Ventricular Assist System. *J Am Coll Cardiol* 2011; 57: 1375-1382.
90. Swedberg K, Komajda M, Bohm M, et al. Ivabradine and outcomes in chronic heart failure (SHIFT): a randomised placebo-controlled study. *Lancet*. 2010; 376: 875–88.

91. Teuteberg JJ, Ewald GA, Adamson RM, et al. Risk assessment for continuous flow left ventricular assist devices: does the destination therapy risk score work? An analysis of over 1,000 patients. *J Am Coll Cardiol* 2012; 60:44–51.
92. Tsao CW, Lyass A, Larson MG, et al. Prognosis of Adults With Borderline Left Ventricular Ejection Fraction. *JACC: Heart Failure* 2016; 4(6): 502-510.
93. Tuzun E, Roberts K, Cohn WE, et al. In Vivo Evaluation of the HeartWare Centrifugal Ventricular Assist Device. *Tex Heart Inst J* 2007; 34: 406-411.
94. Van Der Heijden AC, Levy WC, Van Erven L, et al. Prognostic Impact of Implementation of QRS Characteristics in the Seattle Heart Failure Model in ICD and CRT-D Recipients. *PACE* 2016; 39: 565-573.
95. Verdecchia P, Angeli F, Gattobigio R, et al. Asymptomatic left ventricular systolic dysfunction in essential hypertension: prevalence, determinants, and prognostic value. *Hypertension* 2005; 45: 412–418.
96. Wang TJ, Evans JC, Benjamin EJ, et al. Natural history of asymptomatic left ventricular systolic dysfunction in the community. *Circulation* 2003; 108: 977–982.
97. Wieselthaler GM, O'Driscoll G, Jansz P, et al. for the HVAD Clinical Investigators. Initial clinical experience with a novel left ventricular assist device with a magnetically levitated rotor in a multi-institutional trial. *J Heart Lung Transplant* 2010; 29: 1218-1225.
98. Wong KKL, Tu J, Kelso RM, et al. Cardiac flow component analysis. *Med. Eng. Phys* 2010; 32: 174-188.
99. Wong KKL, Wang D, Ko JKL, Computational medical imaging and hemodynamics framework for functional analysis and assessment of cardiovascular structures. *BioMed Eng OnLine* 2017; 16:35.
100. Yancy CW, Jessup M, Bozkurt B, et al. 2016 ACC/AHA/HFSA Focused Update on New Pharmacological Therapy for Heart Failure: An Update of the 2013 ACCF/AHA Guideline for the Management of Heart Failure. A Report of the American College of Cardiology/American Heart Association Task Force on Clinical Practice Guidelines and the Heart Failure Society of America. *Circulation* 2016; 134: e282-e293.
101. Yancy CW, Jessup M, Bozkurt B, et al. 2013 ACCF/AHA Guideline for the Management of Heart Failure. A Report of the American College of Cardiology Foundation/American Heart Association Task Force on Practice Guidelines. *Circulation* 2013a; 128: e240-e327.
102. Yancy CW, Jessup M, Bozkurt B, et al. 2013 ACCF/AHA guideline for the management of heart failure: a report of the American College of Cardiology Foundation/American Heart Association Task Force on Practice Guidelines. *J Am Coll Cardiol* 2013; 62: e147–e239.
103. Yeboah J, Rodriguez CJ, Stacey B, et al. Prognosis of individuals with asymptomatic left ventricular systolic dysfunction in the Multi-Ethnic Study of Atherosclerosis (MESA). *Circulation* 2012; 126: 2713-2719.